



Marine bivalve shell geochemistry and ultrastructure from modern low pH environments: environmental effect versus experimental bias

S. Hahn¹, R. Rodolfo-Metalpa², E. Griesshaber³, W. W. Schmahl³, D. Buhl¹, J. M. Hall-Spencer², C. Baggini², K. T. Fehr³, and A. Immenhauser¹

¹Inst. of Geology, Mineralogy and Geophysics, Ruhr-University Bochum, Universitätsstraße 150, 44801 Bochum, Germany

²Marine Institute, Marine Biology and Ecology Research Centre, University of Plymouth, A428, Portland Square, Drake Circus, Plymouth, Devon, PL4 8AA, UK

³Dept. of Earth and Environmental Science, Ludwig Maximilian University, Theresienstraße 41, 80333 Munich, Germany

Correspondence to: S. Hahn (sabine.hahn@rub.de)

Received: 20 September 2011 – Published in Biogeosciences Discuss.: 24 October 2011

Revised: 12 April 2012 – Accepted: 29 April 2012 – Published: 29 May 2012

Abstract. Bivalve shells can provide excellent archives of past environmental change but have not been used to interpret ocean acidification events. We investigated carbon, oxygen and trace element records from different shell layers in the mussels *Mytilus galloprovincialis* combined with detailed investigations of the shell ultrastructure. Mussels from the harbour of Ischia (Mediterranean, Italy) were transplanted and grown in water with mean pH_T 7.3 and mean pH_T 8.1 near CO₂ vents on the east coast of the island. Most prominently, the shells recorded the shock of transplantation, both in their shell ultrastructure, textural and geochemical record. Shell calcite, precipitated subsequently under acidified seawater responded to the pH gradient by an in part disturbed ultrastructure. Geochemical data from all test sites show a strong metabolic effect that exceeds the influence of the low-pH environment. These field experiments showed that care is needed when interpreting potential ocean acidification signals because various parameters affect shell chemistry and ultrastructure. Besides metabolic processes, seawater pH, factors such as salinity, water temperature, food availability and population density all affect the biogenic carbonate shell archive.

1 Introduction

Over the last two centuries, human activities have increased the atmospheric CO₂ concentration by about 31 % (Lüthi et al., 2008; Solomon et al., 2009). Approximately one third of the anthropogenic carbon added to the atmosphere is absorbed by the oceans. Uptake of atmospheric CO₂ results in a decrease in ocean water pH, an effect referred to as “ocean acidification” (Caldeira and Wickett, 2003). As a consequence, marine calcareous organisms are increasingly stressed. This is because net calcification rates are affected by decreased calcium carbonate saturation and carbonate ion availability (Fabry et al., 2008; Guinotte and Fabry, 2008; Hall-Spencer et al., 2008).

Previous studies focused on the response of marine calcified organisms to increased CO₂ levels to predict the combined impact of future ocean acidification and increasingly elevated seawater temperatures (Orr et al., 2005; Davies et al., 2007; Fine and Tchernov, 2007; Hoegh-Guldberg et al., 2007; Carroll et al., 2009; Cigliano et al., 2010; Dias et al., 2010; Gutowska et al., 2010; Rodolfo-Metalpa et al., 2010, 2011). Other approaches focussed on past acidification events (Kump et al., 2009; Zeebe and Ridgwell, 2011), such as the Paleocene-Eocene Thermal Maximum 55 million years ago (PETM; Zachos et al., 2005; Sluijs et al., 2007; Iglesias-Rodriguez et al., 2008; Gibbs et al., 2010). Previously applied methods include model organisms cultured under laboratory conditions (e.g. Russell et al., 2004; Kisakürek et al., 2011), mesocosm experiments (e.g. Engel

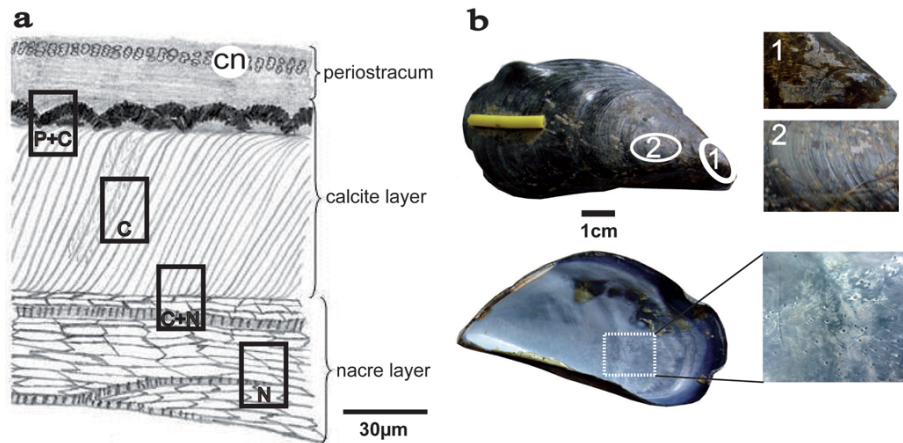


Fig. 1. (a) Sketch of tripartite shell structure of *M. galloprovincialis*. Note periostracum, calcite and aragonitic nacreous layers. The sketch shows the general structure of the shell without a scale. Black boxes indicate sampling sites for isotope analysis. P+C=periostracum and calcite layer; C=calcite layer; C+N=calcite and nacreous layer; N=nacreous layer. “Cn” indicates channel network (“pipe system”) in the upper part of the periostracum. (b) *Mytilus galloprovincialis* from experimental site B1. Note partial lack of periostracum and absence of encrusting or colonizing marine biota in upper image (white circles, labelled 1 and 2, corresponding to close up images to the right) and incomplete nacreous layer with small holes (white rectangle, corresponding to close up image to the right) in lower image. On 26 September 2009, i.e. prior to transplantation, specimens were labelled with a yellow marker in order to differentiate pre- and post-transplantation shell material.

et al., 2005; Riebesell et al., 2007), studies using naturally acidified sites (e.g. Hall-Spencer et al., 2008; Manzello et al., 2008; Kroeker et al., 2011) and the investigation of geological archives (e.g. Mutterlose et al., 2007; Kump et al., 2009; Gibbs et al., 2010). Brief monitoring and culturing experiments (several months to few years; Klein et al., 1996b; Berge et al., 2006; Thomsen et al., 2010) have shortcomings as they provide only limited evidence for longer term adaptation strategies of marine ecosystems (e.g. Guinotte and Fabry, 2008; Ellis et al., 2009; Gutowska et al., 2010). Studies dealing with geological archives suffer from the lack of biological information and are limited by problems of time control (e.g. Ragland et al., 1979; Gomez-Alday and Elorza, 2003; Aubry et al., 2007; Röhl et al., 2007). The majority of geological archive work deals with planktonic organisms from pelagic core material (Raffi et al., 2005; Gibbs et al., 2006; Giusberti et al., 2007; Mutterlose et al., 2007; Westerhold et al., 2007). In contrast, studies with focus on the impact of past acidification events on fossil coastal neritic settings are scarce (Scheibner and Speijer, 2008).

One of the most promising archives of past coastal seawater properties are bivalves (Buick and Ivany, 2004; Lopez Correa et al., 2005; Latal et al., 2006; Foster et al., 2009). Bivalves are sessile organisms that over time record environmental changes in their aragonitic and calcitic shells (Witbaard et al., 1994; Vander Putten et al., 2000; Elliot et al., 2003; Immenhauser et al., 2005; Hippler et al., 2009) and at least their calcitic shells hardparts have, under favourable conditions, a high fossilization potential (Elorza and GarciaGarmilla, 1996; Gomez-Alday and Elorza, 2003; Immenhauser et al., 2005).

The effects of ocean seawater acidification on the bioperformance of the blue mussel *Mytilus edulis* has previously been the topic of mainly biological research (Bamber, 1987; Michaelidis et al., 2005; Berge et al., 2006; Gazeau et al., 2007). The *M. edulis* group, involving the three species *M. edulis*, *M. galloprovincialis* and *M. trossulus* (Koehn, 1991; Aguirre et al., 2006) was investigated for growth patterns (shell length), tissue weight and overall activity and health of these organisms (Bamber, 1987; Berge et al., 2006; Beesley et al., 2008). *Mytilus edulis* has a very wide geographical distribution from the subtropics to the Arctic regions, while *M. trossulus* and *M. galloprovincialis* are more environmentally restricted (Gosling, 2003), but tolerate a wide temperature range (Aral, 1999). The environmental adaptability of *M. edulis* with respect to its wide distribution range including freshwater (Shumway, 1977; Gillikin et al., 2006a, b; Tynan et al., 2006), brackish (Hietanen et al., 1988) and marine settings qualifies the blue mussel as an adaptable and widely used test organism.

Generally, bivalve shells have three layers: the periostracum and two calcium carbonate layers (Fig. 1a). The periostracum forms a quinone-tanned protein layer on the outside of the shell (Fig. 1a; Kennedy et al., 1969), protects the shell, serves as a seal of the extrapallial space for the achievement of supersaturation conditions (Marin and Luquet, 2004) and provides the site of nucleation for calcium carbonate (Checa, 2000). Carbonate shell layers can be distinguished optically as well as by means of their microstructure and mineralogy. The inner layer consists of iridescent, nacreous aragonite (Fig. 1b; Marin and Luquet, 2004) and is composed of 10–20 µm wide tablets that form parallel arranged 0.5 µm

thick lamellae (Fig. 1a). The outer shell layer has a prismatic structure and is composed of calcite prisms (Fig. 1a).

Here we report on the outcome of a study with focus on *M. galloprovincialis* exposed to different seawater pH along a natural gradient in CO₂ levels near volcanic vents (pH_T range 6.6–7.1) off Ischia. We explore and combine the potential of three different proxies within the same carbonate archive: (i) shell isotope and major and trace element geochemistry; (ii) shell ultra- and microstructure imaging, and (iii) crystallographic texture analysis. The aims of this work are twofold. Firstly, we test, the potential of bivalve shell geochemistry and ultrastructure as recorders of environmental change and particularly seawater acidification. Secondly, we assess the sensitivity of the bivalve metabolism to experimental transplantation shock. This work has significance for those concerned in future effects of ocean acidification, paleo-environmental analysis and carbonate archive research in general.

2 Materials and methods

2.1 Field study

The field site lies on the east coast of Ischia (40°43.81' N, 13°57.98' E), south of Castello Aragonese where vents acidify the seawater (Fig. 2). The vents emit gas composed of 90–95 % CO₂, 3–6 % N₂, 0.6–0.8 % O₂, 0.2–0.8 % CH₄ and 0.08–0.1 % Ar and lacked toxic sulphur compounds (Hall-Spencer et al., 2008). Published data of δ¹³C_(CO₂) from gas vents along the eastern margin of Ischia indicate ¹³C-enriched values of +0.5 to –0.8 ‰ (Tedesco, 1996). The seawater pH_T range is 6.6 to 8.1 depending on distance from the vents. Seawater carbon (DIC) isotope values measured during late fall and early winter, i.e. the time interval when the transplantation experiment was undertaken, range from 0.2 ‰ (Ischia harbour, IP, Fig. 2c) to 0.8 ‰ seawater off Ischia (C and OS Fig. 2c, d), whilst a δ¹³C_{DIC} of 0.9 ‰ was found for vent areas (B1 and ES Fig. 2d; Table 1). During spring and summer months, when plankton bloom removes isotopically light carbon from seawater, seawater δ¹³C_{DIC} is more positive (1–1.4 ‰) and differences between harbour, experimental site B1 and control site C are more reduced. During this time, seawater δ¹³C_{DIC} approaches regional values as reported in Pierre (1999).

Ischia seawater oxygen isotope values measured during late fall and early winter, i.e. the time interval when the transplantation experiment was undertaken, range from 1.1 ‰ SMOW (Ischia harbour, IP, Fig. 2c; Table 1) to 1.2 ‰ SMOW seawater at the vent areas (B1 and ES Fig. 2d; Table 1) and off Ischia (C and OS Fig. 2c, d; Table 1). These data are in agreement with regional seawater oxygen isotope values (1.2–1.3 ‰ SMOW) representing April water samples (Pierre, 1999).

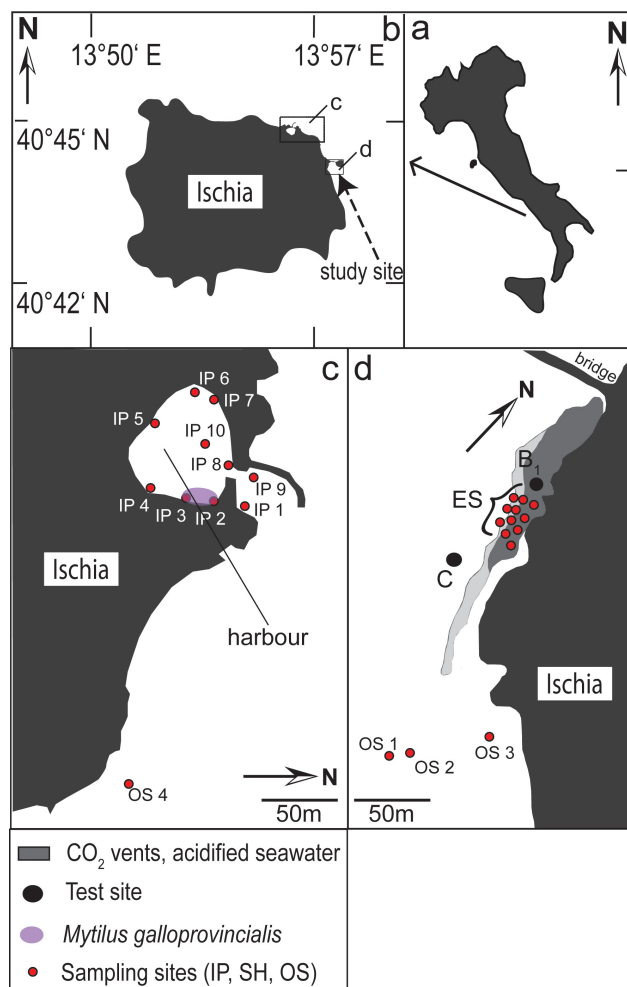


Fig. 2. Map of Italy (a) and the Island of Ischia (b). (c) Schematic map of Ischia harbour with location of the seawater sampling points IP (Ischia Port) and OS (oceanic seawater), as well the location of *M. galloprovincialis*, marked by the purple dot. (d) Schematic map of the natural experiment sites off Ischia in the vicinity of CO₂ vents. Specimens of *M. galloprovincialis* were transplanted in September 2009 from the harbour (pH 8.07) to control site C (mean pH_T 8.07) and experimental site B1 (mean pH_T of 7.25, minimum pH_T 6.83) where they were kept until December 2009 (modified after Hall-Spencer et al., 2008). Seawater sampling sites are labelled OS and ES.

Several adult *M. galloprovincialis* (>40 mm length) collected from the Ischia port (pH_T 8.07) (Fig. 2b, c) were transplanted to a control site with normal pH_T (C in Fig. 2b, d; mean pH_T 8.07) and to an experimental site with acidified seawater (B1 in Fig. 2b, d; mean pH_T 7.25, minimum pH_T 6.83). Samples were labelled with a yellow marker glued onto the shell edge (Fig. 1b) to differentiate between shell precipitated before and after transplantation. The mussels were kept at the test sites for 68 days (28 September to 2 December 2009). Seawater temperature, pH_T and total alkalinity (At) were monitored for the duration of the experiment

Table 1. Parameters of harbour and field experimental sites. Mean \pm S.D. seawater chemistry calculated over the experiment period at the experimental site B1 and control site C. pH_T is in total scale; pCO_2 in μatm ; HCO_3^- , CO_3^{2-} , CO_2 and DIC (dissolved inorganic carbon) are in $\mu\text{mol kg}^{-1}$; saturation state (Ω) of aragonite and calcite. IP = Ischia port (harbour); OS = ocean seawater off Ischia; ES = experimental site.

	mean T ($^{\circ}\text{C}$) late summer to early winter	pH_T	pCO_2 (μatm)	HCO_3^- ($\mu\text{mol kg}^{-1}$)	CO_3^{2-} ($\mu\text{mol kg}^{-1}$)	CO_2 ($\mu\text{mol kg}^{-1}$)	DIC ($\mu\text{mol kg}^{-1}$)	Ω calcite	Ω aragonite	$\delta^{18}\text{O}$ (‰ SMOW) late fall/ early winter	$\delta^{13}\text{C}$ (‰ VPDB) late fall/ early winter	$\delta^{18}\text{O}$ (‰ SMOW) spring	$\delta^{13}\text{C}$ (‰ VPDB) spring
Harbour (IP)	18.9 (± 0.98)	8.07 (± 0.07)	n.d.	2993 (± 136)	n.d.	n.d.	n.d.	n.d.	n.d.	1.1 (± 0.02)	0.2 (± 0.02)	1.2–1.3 (± 0.02)	1.4 (± 0.02)
Site C (OS)	21 (± 4.2)	8.07 (± 0.04)	474 (± 58)	2015 (± 74)	235 (± 35)	15 (± 2)	2265 (± 43)	5.42 (± 0.74)	3.55 (± 0.52)	1.2 (± 0.02)	0.8 (± 0.02)	1.2–1.3 (± 0.02)	1.4 (± 0.02)
Site B1 (ES)	20.7 (± 4.2)	7.25 (± 0.44)	5494 (± 5520)	2428 (± 108)	61 (± 45)	173 (± 175)	2661 (± 226)	1.37 (± 0.95)	0.98 (± 0.69)	1.2 (± 0.02)	0.9 (± 0.02)	1.2–1.3 (± 0.02)	1.4 (± 0.02)

(Table 1). Refer to Hall-Spencer et al. (2008), Martin et al. (2008), Cigliano et al. (2010) and Rodolfo-Metalpa et al. (2010) for details of the experimental and analytical approach.

2.2 Methods: carbon and oxygen isotope and elemental geochemistry

Carbon and oxygen-isotope analyses of 170 powder samples of *M. galloprovincialis*_{B1} and C (Table S1, Supplement) extracted from mussel shells and 28 seawater samples were performed with a ThermoFinnigan MAT 253 ratio mass spectrometer equipped with a Gasbench II at the isotope laboratory of the Institute for Geology, Mineralogy and Geophysics (Ruhr-University Bochum, Germany). Repeated analyses of certified carbonate standards (NBS 19, IAEA CO-1 and CO-8) and internal standards show an external reproducibility of $\leq 0.02 \text{‰}$ for $\delta^{13}\text{C}$ and $\leq 0.06 \text{‰}$ for $\delta^{18}\text{O}$ for the powder samples. An internal laboratory standard (Na_2CO_3) was used for the seawater $\delta^{13}\text{C}_{\text{DIC}}$ samples. The 1σ -reproducibility of the measured values is 0.19‰ $\delta^{13}\text{C}_{\text{DIC}}$. All isotope results are reported in per mil (‰) relative to the V-PDB standard in the conventional manner. For analyses of the seawater $\delta^{13}\text{C}_{\text{DIC}}$ vials were treated with 85 % phosphoric acid and then flushed with helium. Subsequently, carbonate hardness was determined and the required amount of sample material was added into the prepared vials. Seawater $\delta^{18}\text{O}$ was analyzed in the laboratories of Johanneum Research Centre in Graz (Austria). Seawater $\delta^{13}\text{C}_{\text{DIC}}$ and $\delta^{18}\text{O}$ from Ischia harbour, control and experimental sites are given in Table 1.

In total two different sampling approaches were applied for powder samples. One approach used bulk shell samples (including all shell layers and shell layers in variable admixtures; Fig. 1a) following a transect along the maximum growth axis of the shell. For the second approach, shells were cut perpendicularly to the maximum growth axis and calcite samples were extracted using a micro drilling system (MicroMill, MechanteK (esi/New Wave); Dettman and Lohmann, 1995). For detailed information of the analytical procedure refer to Immenhauser et al. (2005). For the sake of data comparability, aragonitic (nacreous) layer iso-

tope data were normalized against calcite isotope values using the equation of Rubinson and Clayton (1969) for $\delta^{13}\text{C}$ and that of Tarutani et al. (1969) for $\delta^{18}\text{O}$.

Elemental geochemistry analysis was performed on a *M. galloprovincialis* shell from experimental locality B1 (Fig. 2b, d) using a Cameca SX50 electron microprobe at the Department of Earth and Environmental Sciences of the LMU Munich; Germany. The probe was operated at 15 keV acceleration and 20 nA beam current. Barium (Ba), calcium (Ca), chlorine (Cl), iron (Fe), magnesium (Mg), manganese (Mn), phosphorus (P), silicon (Si), sodium (Na) and strontium (Sr) were measured. Albite (Na), apatite (Ca and P), baryte (BaSO_4) (Ba), Fe_2O_3 (Fe), ilmenite (MnTiO_3) (Mn), periclase (Mg), SrSO_4 (Sr), vanadite (Cl) and wollastonite (Si) were used as standards. Matrix correction was performed by the PAP procedure (Pouchou and Pichoir, 1984). The reproducibility of standard analyses was $< 1 \%$ for each routinely analysed element. The PAP corrected data were stoichiometrically calculated as carbonate. Samples were taken over the entire shell, but emphasis was placed on the shell formed directly before and after the transplantation (Fig. 1b).

2.3 Methods: shell microstructure and texture analysis

The microstructure and texture of *M. galloprovincialis* shells were investigated under a scanning electron microscope (SEM) using polished thin sections and fragments of surface samples as well as under electron backscattered diffraction (EBSD). We use the following macroscopic reference frame: all sample wafers were obtained from a longitudinal cut through the shell that ranged from the hinge to the commissure of the valve. The sample wafers were ~ 200 micrometer thick and placed 90 degrees to the plane of cut onto a glass holder. Samples were subsequently prepared on both sides of the shell as highly polished, 150 μm thick sections. The surface of the thin sections was subsequently etched for 45 s with a suspension of alumina nanoparticles. The samples were then cleaned, dried, and coated with the thinnest possible conducting carbon coating (SEM: 4–6 μm and EBSD: 15 μm). Scanning electron micrographs and EBSD patterns were obtained on a LEO Gemini 1530 SEM and a JEOL

Table 2. Thickness characteristics of different shell layers of *M. galloprovincialis*_{B1} and C in μm . Shell thickness was measured before and after transplantation. N.d. = no data; n.f. = not formed, i.e. shell was not precipitated.

	<i>Mytilus galloprovincialis</i> from site C pH_T 8.07 in μm	<i>Mytilus galloprovincialis</i> from site B1 pH_T 7.25 in μm
Calcite layer	130–500	215–820
– commissure	200–250	215–230
– near commissure (after transplantation, C and B1)	200–250	340–430
– transition from harbour site to experimental site	n.d.	620
– near commissure (before transplantation, C and B1)	500	760–820
– middle of the shell	130	430–520
Nacreous layer	5–440	10–150
– commissure	0–10	n.f.
– near commissure (after transplantation, C and B1)	0–10	n.f.
– transition from the harbour site to experimental site	n.d.	n.f.
– near commissure (before transplantation, C and B1)	40	10–150
– middle of the shell	440	10–100
Total shell (calcite and nacreous layer)	135–570	225–970
– commissure	200–260	215–230
– near commissure (after transplantation, C and B1)	200–260	340–430
– transition from the harbour site to experimental site	n.d.	620
– near commissure (before transplantation, C and B1)	540	770–970
– middle of the shell	570	440–620

JSM 6500F SEM each equipped with the HKL Technology “Channel 5” EBSD system. Images and EBSD patterns were generated using an accelerating voltage of 20 kV and a beam current of 3.0 nA. The lattice orientation of grains was determined with a spatial resolution of 2–3 μm and an absolute angular resolution of ± 0.5 degrees. Electron backscattered diffraction patterns with a mean angular uncertainty of 1 degree and above were discarded. Several EBSD maps were conducted from each wafer, starting at the commissure and moving towards the hinge. Calcite c-axes of the pole figures always point to the outer rim of the shell and rotate (for the calcitic shell portion) with the curvature of the shell.

3 Results

3.1 Macroscopic observations

Macroscopic examination of *M. galloprovincialis*_{B1} samples transplanted to the acidified experimental site (pH_T 7.25, Fig. 2d) developed characteristic features of the periostracum, the calcitic and the aragonitic shell layers: (i) Mussels lacked encrusting or colonizing marine biota (Fig. 1b); (ii) near the umbo, the oldest part of the shell, the periostracum was abraded while (iii) the nacreous layer lacked its normal lustre and was pitted with small holes (~ 0.1 mm) and scattered with white spots (Fig. 1b). In contrast, *M. galloprovincialis*_C from the control site C (pH_T 8.07) were characterized by shells encrusted by marine biota and displayed a lustrous nacreous layer.

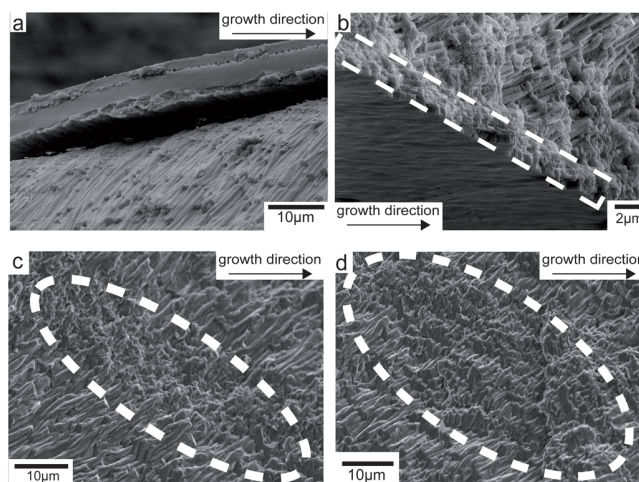


Fig. 3. Calcite layer SEM images from *Mytilus galloprovincialis*_{B1} and C fragments of the surface. Images are from outer margin precipitated from normal marine seawater pH (a, b) and from shells precipitated from acidified seawater (c, d). (a and b) Calcite layer of *M. galloprovincialis* from control site C ($\text{pH}_T = 8.07$). Note well structured calcite layer. White stippled box indicates aragonite layer. (c and d) Calcite layer of *M. galloprovincialis* from acidified experimental site B1. Note portions of calcite layer with disorganized shell structure (white stippled oval) within otherwise well organized calcite shell.

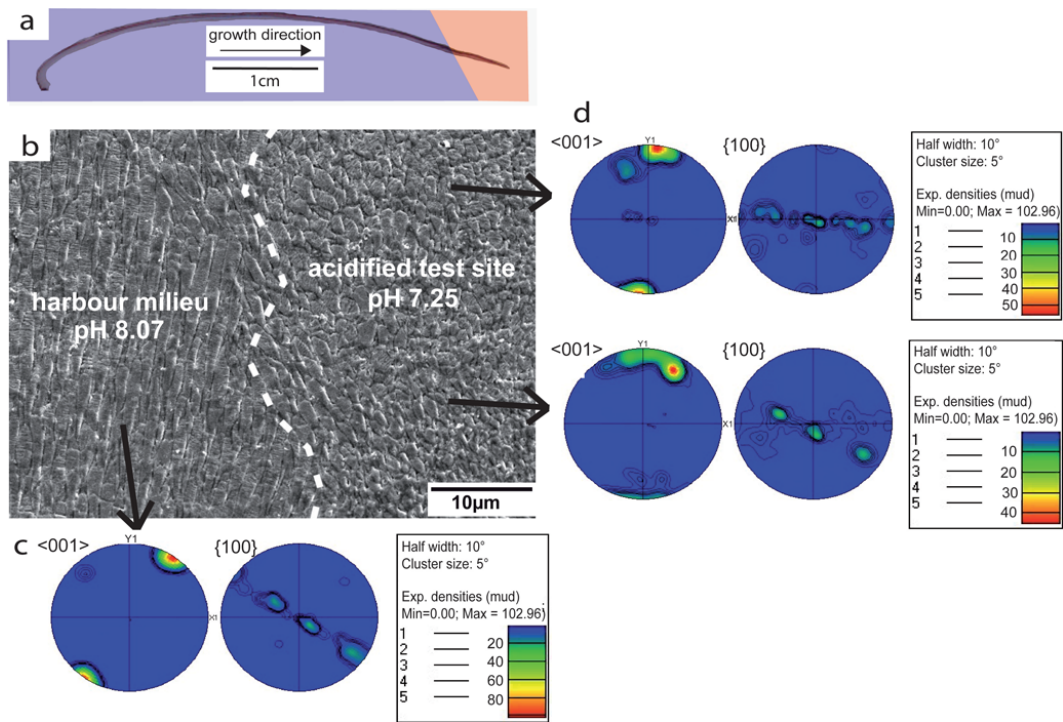


Fig. 4. Thin section view of calcite layer of *M. galloprovincialis* from acidified seawater site B1. **(a)** Blue colour indicates shell precipitated prior to transplantation and red colour indicates shell precipitated after transplantation to acidified test site B1. **(b)** SEM image of shell precipitated parallel to the longest growth axis and directly before and after transplantation. Note pronounced differences in the orientation of the calcite layer across transplantation event (white, stippled line). Locations of respective pole figures **(c)** and **(d)** are indicated. **(c)** and **(d)** Pole figures representing stereographic projections of crystallographic axes and planes. The strength of clustering is specified with the MUD (multiples of uniform density) value that gives the distribution pattern of EBSD data relative to that of a random distribution.

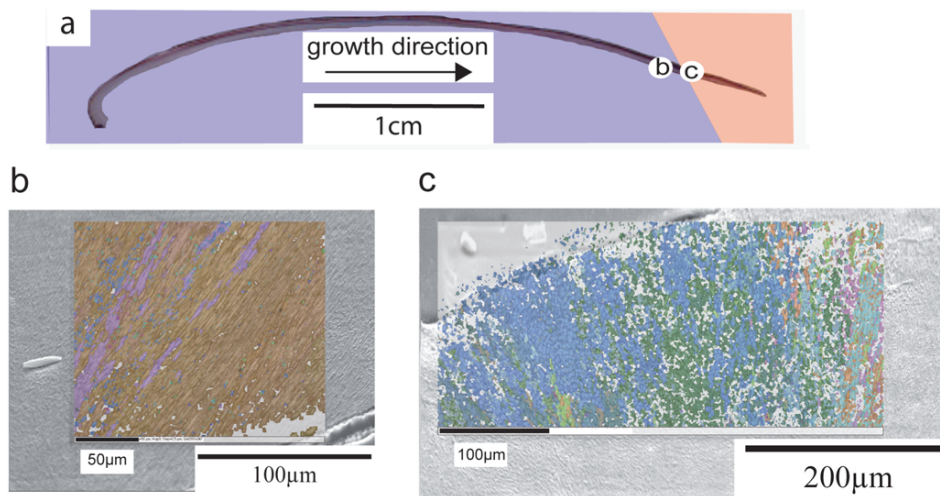


Fig. 5. Thin-section view of *M. galloprovincialis* from experimental site B1. **(a)** Blue colour indicates shell precipitated prior to transplantation and red colour indicates shell precipitated after transplantation to acidified experimental site. **(b)** and **(c)** Electron backscattered diffraction (EBSD) maps. Note location of b and c in Fig. 5a. Different colours indicate different orientations of calcite prisms. White points denote those regions within the shell where Kikuchi patterns could not be indexed. The three RGB colour components code for the three Euler angles of crystal orientation. In order to visualize all patterns the whole range of Euler angles are plotted (Euler 1 between 0–180°, Euler 2 between 0–180° and Euler 3 between 0–120°). Note rather homogenous (brown to lilac, **b**) colours in well structured calcite shell prior to transplantation. The EBSD map of shell portions precipitated after the transplantation indicates a wider range of colours and spatially disorganized calcite prisms indicating shell precipitation under acidified environments.

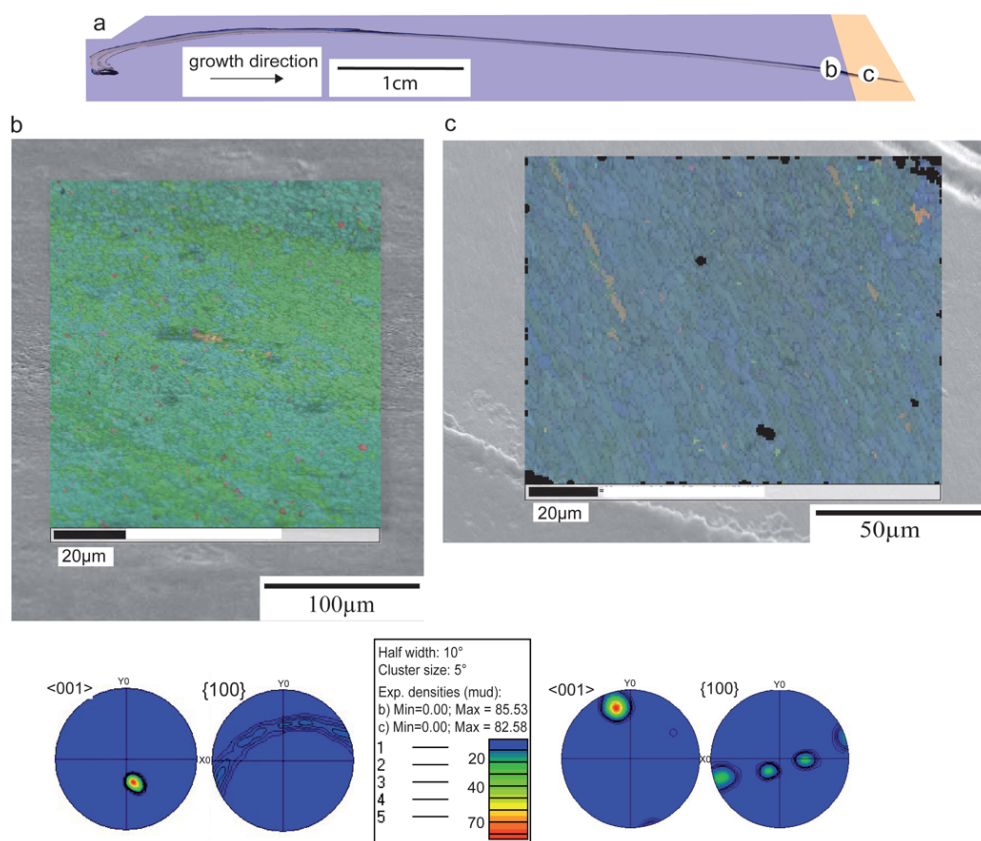


Fig. 6. Thin-section view of *M. galloprovincialis* from control site C. **(a)** Blue colour indicates shell precipitated prior to transplantation and orange colour indicates shell precipitated after transplantation to control site. **(b and c)** Electron backscattered diffraction (EBSD) maps and pole figures. Note location of b and c in Fig. 6a. Different colours indicate different orientations of calcite prisms. Black points denote those regions within the shell where Kikuchi patterns could not be indexed. The three RGB colour components code for the three Euler angles of crystal orientation. In order to visualize all patterns the whole range of Euler angles are plotted (Euler 1 between 0–180°, Euler 2 between 0–180° and Euler 3 between 0–120°). Note homogenous (green to blue) colours in well structured calcite shell prior to and after transplantation. The differences between the maps are due to different step sizes. Pole figures representing stereographic projections of crystallographic axes and planes. MUD = Multiples of Uniform Density.

3.2 Shell ultrastructure, microstructure and texture

Figure 1a displays a sketch of the major structural units of the shell's ultrastructure based on SEM observations of transplanted *M. galloprovincialis*_{B1} and C. In the following, differences and similarities of shell portions that represent the pre-transplantation growth period and such that represent the post-transplantation growth period are compared.

The thickness of the calcite and aragonite layers varies significantly over the life time of individual specimen whilst the thickness of the periostracum remains more constant. The calcite shell ranges from 120 to 830 μm and the nacreous layer ranges from 5 to 1520 μm in thickness (Table 2). The calcite shell layer formed from seawater at sites B1 and C has thinned to about 70 % in the case of experimental site *M. galloprovincialis*_{B1} and to about 55 % of its former thickness in the case of control site *M. galloprovincialis*_C (Table 2). In *M. galloprovincialis*_{B1} the nacreous shell layer was not formed,

while it is present in samples from site C as a 5–10 μm thick layer (Table 2).

Figure 3 depicts comparable portions of *M. galloprovincialis*_{B1} and C shells formed after the transplantation. The calcite layer of samples from control site seawater pH environments (Site C, pH_T 8) is well ordered (Fig. 3a to b), while, in contrast, the calcitic layer of the *M. galloprovincialis*_{B1} specimen from the acidified experimental site (pH_T of 7.25) is unordered. This effect is most pronounced in the portion of the shell formed directly after the transplantation into the acidified environment (Fig. 4b). With time, the shell structure formed under acidified seawater conditions takes up the formerly structured organization, albeit with localized patches of disordered shell calcite prisms (Fig. 3c and d). The later observation is considered significant.

Electron backscattered diffraction measurements from *M. galloprovincialis*_{B1} are displayed in Figs. 4 and 5. The SEM image in Fig. 4b shows the shell's microstructure across the

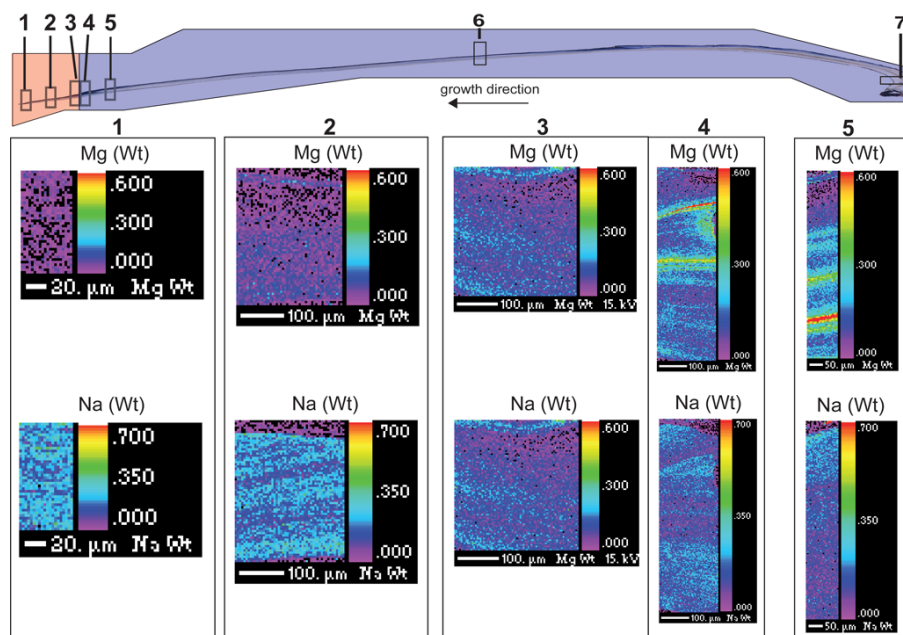


Fig. 7. Thin section view of *M. galloprovincialis* from acidified experimental site B1. Blue colour indicates shell precipitated prior to transplantation and red colour indicates shell precipitated after transplantation. Gray boxes numbered 1 through 7 indicate the position of the microprobe maps. The maps 1 to 5 were measured across the calcitic shell layer only. Maps 6 and 7 are shown in Fig. 8 and are located at the mid-shell and the hinge. Map 6 was measured across the calcitic and aragonitic layers, map 7 was measured across the aragonitic layer. Magnesium and sodium microprobe maps 1 through 5 are numbered in ascending order from the commissure to the hinge (corresponding to the boxes with the microprobe maps). Due to the incisive difference between the element magnesium (Mg) and sodium (Na), these elements are illustrated. The concentration of elements is given in weight percent (Wt). The element distribution in the shell displays no discernible pattern while concentrations of Mg and Na follow opposite trends.

transition from normal to acidified seawater. Calcite prisms formed prior to the transplantation are aligned in parallel (Fig. 4b) and the corresponding electron backscattered diffraction pattern shows a unimodal distribution (Fig. 4c). After the transplantation, a microstructural disarrangement of the shell fabric is observed (Fig. 4b). This feature is perhaps best explained as an adaptation shock of the mussel to the transplantation. After adaptation to the new environment, *M. galloprovincialis*_{B1} precipitates an ordered but thinner calcite shell layer with prisms arranged in parallel (Fig. 3c, d). The electron backscattered diffraction projection patterns in Fig. 4d, documenting post-transplantation shell growth, display bimodal, or more distribution.

The shell texture, specifically the 3-D orientation of calcite fibre c-axes, displays a similar transplantation effect (Fig. 5). A well ordered array of calcite fibre c-axes is precipitated prior to the transplantation (Fig. 5b). Less ordered fibre c-axes characterize the portion of the shell formed directly after the transplantation (Fig. 5c).

Electron backscattered diffraction analyses of control site *M. galloprovincialis*_C are displayed in Fig. 6. The shell texture, specifically the 3-D orientation of calcite fibre c-axes, displays a well ordered array precipitated prior and after transplantation (Fig. 6b and c). Electron backscattered

diffraction projection patterns in Fig. 6b and c show a unimodal distribution.

3.3 Shell geochemistry

3.3.1 Elemental abundances

Microprobe analysis results of samples obtained from *M. galloprovincialis*_{B1} are listed in Table S2 (Supplement). Magnesium and sodium abundances are summarized in seven distribution pattern maps shown in Figs. 7 and 8. Clear differences in Ca, Mg, Na and P elemental composition between shell portions representing normal control site and such representing acidified experimental site seawater are recognized. All other elements were either evenly distributed or below detection limit.

While Ca values are around 390 000 ppm (39 wt %) in all measured maps, P shows a highly variable concentration distribution pattern of 1510 (0.151 wt %) to 4680 ppm (0.468 wt %). Both elements, however, are enriched in the calcite in comparison to the aragonite layer. Magnesium and sodium show opposing distribution patterns. While magnesium is only present in the calcite layer, sodium is present in both layers. In contrast to magnesium, however, sodium is more abundant in the nacreous layer (10 600 ppm or

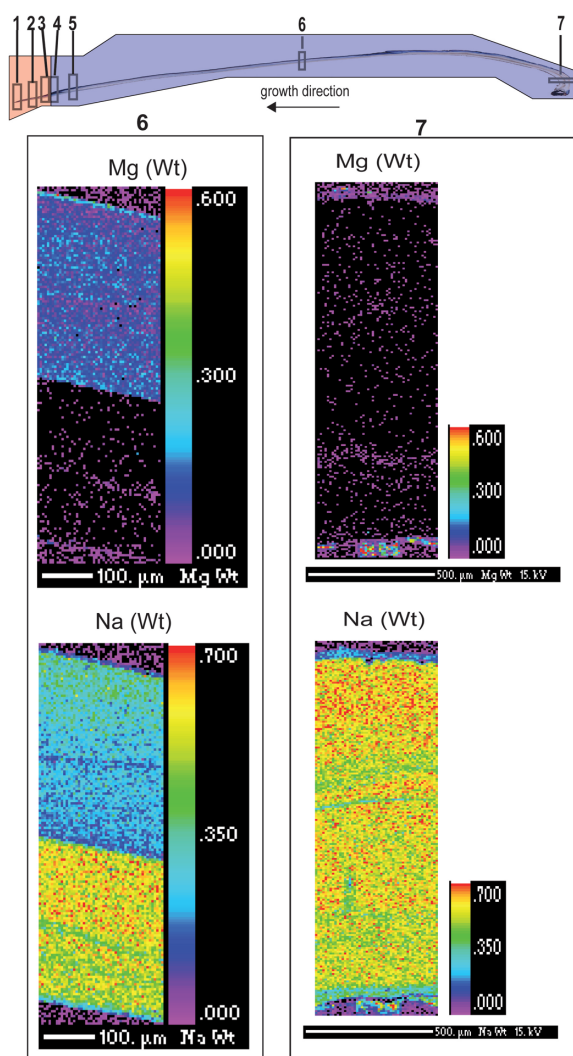


Fig. 8. Thin section view of *M. galloprovincialis* from acidified experimental site B1. Blue colour indicates shell precipitated prior to transplantation and red colour indicates shell precipitated after transplantation to acidified test site. Gray boxes numbered 1 to 7 indicate the position of the microprobe maps. The maps 1 to 5 are shown in Fig. 7. Magnesium and sodium concentration is given in weight percent. Differences in element concentrations in map 6 reflect differences between calcite and aragonite layer. Magnesium and sodium are incorporated in calcite layer. Nacreous layer displays considerably higher concentrations of sodium. Judging from elemental maps, the shell hinge is composed almost entirely of aragonite.

1.060 wt %) compared to the calcite layer (about 4500 ppm or 0.450 wt %; Table S2). The sodium content decreases gradually from the shell hinge to the most recent portions of the shell.

Magnesium shows a different distribution pattern with increasing and decreasing trends between shell hinge and commissure. In part, this distribution is related to the thickness of the aragonite versus the calcite layer with Mg incorporated

far more substantially into calcite. Initially, Mg increases in abundance from the shell hinge towards the commissure, this as the nacreous shell layer thins whilst the calcitic layer thickens (Table S2). At the commissural end of the shell (i.e. in the youngest portions of the shell), Mg abundances within the calcite layer first increase and then decrease.

3.3.2 Carbon and oxygen isotope ratios from specific shell layers

In order to assess the relative significance of each individual shell layer (periostracum, calcite layer, nacreous/aragonite layer) on bulk $\delta^{13}\text{C}$ and $\delta^{18}\text{O}$ isotope data and in order to capture the internal variability, sub-samples were drilled from individual layers in selected shells (Fig. 1a). Isotope data are listed in Table S1 (Supplement) and shown in Fig. 9 whilst seawater isotope values are given in Table 1. Due to the complexity of the data set, the main features are summarized below. Previous work by Rubinson and Clayton (1969; $\delta^{13}\text{C}$) and Tarutani et al. (1969; $\delta^{18}\text{O}$) reported on the crystallographical effects of isotope fractionation in inorganic aragonite and calcite precipitates. Therefore, $\delta^{13}\text{C}_{\text{Aragonite}}$ values in Fig. 9a and c were normalized for calcite. In a comprehensive study, however, Lecuyer et al. (2004) found no evidence that oxygen isotope fractionation between mollusc aragonite and water differs from that of mollusc calcite and water. Aragonite oxygen-isotope values in Fig. 9b and d were normalized by the much smaller factor of 0.06 ‰ as proposed in Tarutani et al. (1969) but it seems unclear if this step is justified for biogenic carbonates.

Bulk carbon isotope values from *M. galloprovincialis*_{B1} shells prior to transplantation range from -1.6 to -0.2 ‰ (standard deviation (σ) = 0.02 ‰). Calcite and aragonite $\delta^{13}\text{C}$ ratios scatter between 1.3 and -0.3 ‰ (σ = 0.02 ‰). Shell material from experimental site B1 (pH_T 7.25) has $\delta^{13}\text{C}$ values of 2.4 ‰ (σ = 0.02 ‰) (with periostracum) and around 2.0 ‰ (σ = 0.02 ‰) (without periostracum), i.e. a difference of less than 0.5 ‰.

Furthermore, *M. galloprovincialis*_{B1} and C values reveal differences between the three layers (Fig. 9 and Table S1). The lightest $\delta^{13}\text{C}_{\text{shell}}$ values were recorded in the nacre-layer. Samples combining calcite and nacreous layer are enriched in ^{13}C . The values combining periostracum and calcite layer and such data from the calcite layer alone are intermediate in isotopic composition. This pattern is not always detectable in *M. galloprovincialis* from sites B and C. Furthermore, sub-samples combining (i) periostracum and calcite layer and (ii) calcite and nacreous layer show an ontogenetic trend to higher values from the hinge to the commissure, i.e. in growth direction.

Oxygen isotope ratios were analyzed from sub-samples drilled from individual layers in selected shells (Fig. 1a) as well as from bulk samples. Results are shown in Table S1 and summarized in Fig. 9. Bulk $\delta^{18}\text{O}$ data from *M. galloprovincialis*_{B1} formed prior to transplantation range from

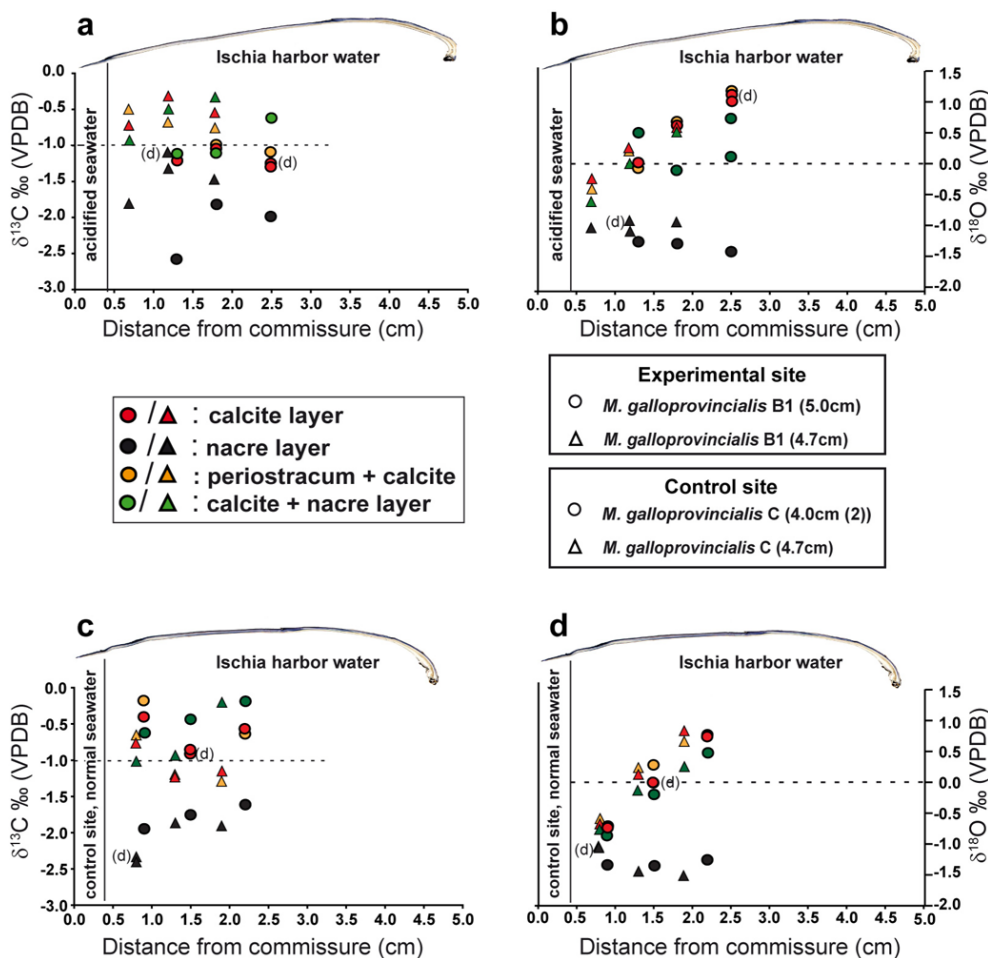


Fig. 9. Differential carbon and oxygen isotope ratios representing shell layer and mixed samples (legend and Fig. 1a) of four specimens of *M. galloprovincialis* B1 and C (a–d) plotted against distance from commissure. Different specimen are characterized by their different shell length and experimental site, e.g. *M. galloprovincialis* C (4.0 cm, 2) refers to a specimen with a shell length of 4 cm that was dislocated to control site C. Isotope values from two specimen from the same site, differentiated by their length, are labelled by a circle and a triangle, respectively. (a through d) *Mytilus galloprovincialis* shell isotope values from experimental site B1 (a, b) and control site C (c, d). Colour code represents different layers analyzed. Note considerable differences in isotope values from different shell layers. Aragonitic (nacreous) layer isotope data were normalized against calcite isotope values using the equation of Rubinson and Clayton (1969) for $\delta^{13}\text{C}$ and that of Tarutani et al. (1969) for $\delta^{18}\text{O}$.

–0.4 to 0.6 ‰ ($\sigma = 0.02$ ‰). Without periostracum material, data range from –0.3 to 0.6 ‰ ($\sigma = 0.02$ ‰). In shell material precipitated under acidified seawater conditions, $\delta^{18}\text{O}$ bulk ratios are in the order of 0.8 ‰ ($\sigma = 0.01$ ‰). In samples lacking periostracum material, lower values of 0.6 ‰ ($\sigma = 0.02$ ‰) are found. All of these values are depleted in ^{18}O relative to the $\delta^{18}\text{O}_{\text{seawater}}$ of 1.2 ‰ SMOW.

Furthermore, *M. galloprovincialis*_{B1} and C values reveal isotopic differences between shell layers (Fig. 9 and Table S1), with the nacreous layer being depleted. From the oldest shell portions (hinge) to the youngest shell portions (commissure) $\delta^{18}\text{O}$ values decrease. This includes samples taken from (i) the periostracum and the calcite layers, (ii) samples from the calcite layer and (iii) samples drilled from the cal-

cite and nacreous layers (Fig. 9). In contrast, samples drilled within the transect in the nacreous layer remain invariant.

3.3.3 Isotope time series analysis of calcite shell samples: acidified versus normal seawater environments

In order to capture the geochemical pattern contained in shell material across the transplantation interval, a high resolution isotope record focusing on the calcite layer of *M. galloprovincialis*_{B1} and *M. galloprovincialis*_C was analyzed. Data are listed in Table S1 (Supplement) and results are displayed in Fig. 10. The data set is complex but clearly indicates that fractionation patterns in different shell layers of the same mussel differ considerably. The main features are

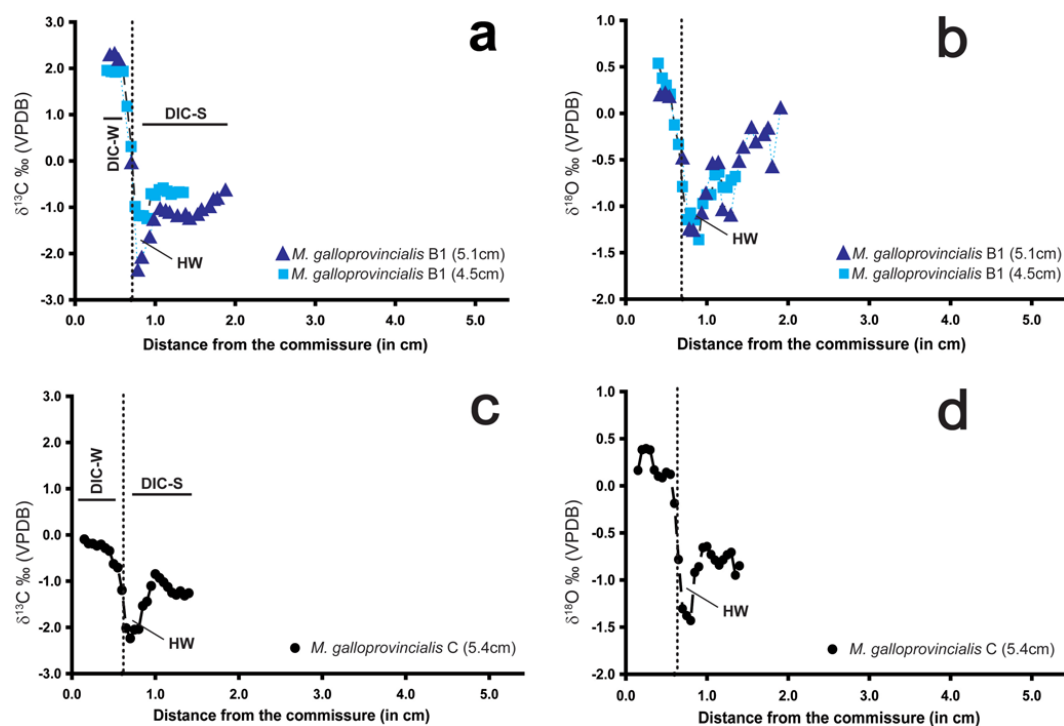


Fig. 10. Time series $\delta^{13}\text{C}$ and $\delta^{18}\text{O}$ ratios plotted against distance from shell commissure. Different specimens/shells are labelled according to shell length. *Mytilus galloprovincialis*_C (5.4 cm) refers, for example, to a specimen with shell length of 5.4 cm transplanted from the harbour to the control site C. (a and b) Horizontal, black stippled line separates data from shell material precipitated before (right) and after (left) transplantation. Note considerable negative excursion in both carbon and oxygen data in August 2009 followed by marked positive trend until December 2009. Negative $\delta^{18}\text{O}$ shift is probably best interpreted as effect of an anomalous warm and long heat-wave (HW). Positive shift is only in part related to temperature alone and is probably related to seawater pH change and metabolic effects. DIC-S refers to seawater $\delta^{13}\text{C}_{\text{DIC}}$ value during summer 2009 and DIC-W the $\delta^{13}\text{C}_{\text{DIC}}$ value of seawater during winter 2009. (c and d) Data from *M. galloprovincialis*_C showing transition from Ischia harbour to normal pH control site C. Near identical isotope pattern as recorded at site B1 is found albeit with smaller amplitudes.

summarized below and are placed against seawater values as shown in Table 1.

Calcite layer carbon and oxygen isotope ratios of *M. galloprovincialis*_{B1} prior to transplantation range from -2.4 to -0.6 ‰ ($\delta^{13}\text{C}_{\text{shell}}$; $\sigma = 0.02$ ‰) and -1.4 to 0.1 ‰ ($\delta^{18}\text{O}_{\text{shell}}$; $\sigma = 0.03$ ‰). Isotope ratios of shell material precipitated directly after the transplantation, are enriched in ^{13}C and range between 0 and 0.3 ‰ ($\sigma = 0.02$ ‰) and ^{18}O (-0.1 and -0.5 ‰; $\sigma = 0.03$ ‰). In calcite precipitated after the adaptation of the shell to acidified seawater at experimental site B1 (Fig. 2b, d), strongly elevated $\delta^{13}\text{C}$ ratios of 1.9 to 2.4 ‰ ($\sigma = 0.02$ ‰) and $\delta^{18}\text{O}$ ratios of 0.2 to 0.5 ‰ ($\sigma = 0.03$ ‰) are found. The maximum difference in pre- and post-transplantation $\delta^{13}\text{C}$ calcite layer is in the order of 4 ‰ and around 1.9 ‰ for $\delta^{18}\text{O}$. This difference is considerable. The maximum difference in pre- and post-transplantation $\delta^{13}\text{C}$ bulk shell materials is smaller, i.e. up to 2.5 ‰ and about 1.0 ‰ for $\delta^{18}\text{O}$.

Carbon and oxygen isotope ratios of *M. galloprovincialis*_C prior to transplantation range from -2.2 to -0.9 ‰ ($\delta^{13}\text{C}_{\text{shell}}$; $\sigma = 0.02$ ‰) and -1.4 to -0.9 ‰ ($\delta^{18}\text{O}_{\text{shell}}$; $\sigma =$

0.03 ‰). Shell material precipitated after the adaptation to the normal seawater conditions at control site C (Fig. 2b, d) ranges between -0.7 to -0.1 ‰ ($\delta^{13}\text{C}_{\text{shell}}$; $\sigma = 0.02$ ‰) and $\delta^{18}\text{O}$ ratios of 0.1 to 0.4 ‰ ($\sigma = 0.03$ ‰). The maximum difference in pre- and post-transplantation $\delta^{18}\text{O}$ calcite layer is around 1.8 ‰ (2 ‰ for $\delta^{13}\text{C}_{\text{calcite}}$), i.e. about 50 % of the difference found in shells kept under acidified conditions. For bulk samples, the maximum difference in pre- and post-transplantation $\delta^{13}\text{C}_{\text{shell}}$ is 1.4 ‰ and around ~ 1.6 ‰ for $\delta^{18}\text{O}_{\text{shell}}$.

4 Interpretation and discussion

4.1 Sensitivity of *Mytilus* shell geochemistry and ultrastructure to environmental change

All mussels of the *M. edulis* group show a distinct biological control on biomineralization (Heinemann et al., 2008) and, in their rather complex, tripartite shell structure (Fig. 1), a high level of mineralogical and geochemical complexity. The data shown here are clear evidence that this internal complexity is

underexplored from the viewpoint of geochemistry and crystallography and represents a significant obstacle for those dealing with the paleo-environmental analysis of fossil material.

Additional complexity comes from the metabolic effects active during the incorporation of carbonate ions from seawater and organic matter taken up as food and incorporated as bicarbonate ions into the bivalve shells (Lorens and Bender, 1977; Klein et al., 1996a, b; Vander Putten et al., 2000; Lecuyer et al., 2004; Dalbeck et al., 2006; Wanamaker et al., 2007; Heinemann et al., 2008). During winter months, Ischia harbour seawater $\delta^{13}\text{C}_{\text{DIC}}$ is considerably depleted (mean of 0.2 ‰) due to sewage water from Ischia Porto village. Lowest DIC carbon isotope values of -0.5 ‰ (and $\delta^{18}\text{O}_{\text{seawater}}$ of 0.8 ‰ SMOW) were measured from a water sample taken directly beside one of the sewage pipes in the harbour. During much of spring to early fall, when biogenic carbonate secretion preferentially removes ^{12}C from seawater, mean harbour DIC values reach 1 ‰ and more (DIC-S in Fig. 10a, c). In late fall and winter months, seawater $\delta^{13}\text{C}_{\text{DIC}}$ of the control site C is in the order of 0.8 ‰ (DIC-W in Fig. 10c), whilst it is 0.9 ‰ near the vent areas (DIC-W in Fig. 10a; cf. Fig. 2d and Table 1). The slightly more positive seawater $\delta^{13}\text{C}_{\text{DIC}}$ at the acidified experimental site B1 (Fig. 10a) is probably due to the ^{13}C -enriched values of the volcanic CO_2 (Tedesco, 1996). During spring and summer months control (C) and experimental site (B1) seawater values approach the regional values of 1.2 to 1.4 ‰ reported in Pierre (1999).

Mussels were transplanted near end of September and moved to the control and the experimental sites (Fig. 2d). Bivalves experienced an approximate $\Delta^{13}\text{C}_{\text{DIC}}$ of about 0.4 ‰ from Ischia harbour (spring and summer, ^{12}C -depleted) to the test and experimental site (late fall to winter months, ^{12}C -enriched). Shell $\delta^{13}\text{C}_{\text{calcite}}$ values are depleted by about 1.5 to 2 ‰ relative to pre-transplantation harbour seawater $\delta^{13}\text{C}_{\text{DIC}}$ conditions of 0.8 to 1 ‰ (Fig. 10a, c). Following previous work (Vander Putten et al., 2000; Wanamaker et al., 2007; Immenhauser et al., 2008), this depletion is indicative of metabolic processes and an organic carbon source. Directly prior to the transplantation event, shell $\delta^{13}\text{C}_{\text{calcite}}$ shifts to even more depleted values (HW in Fig. 10). We propose that mussels suffered from an anomalous warm and long heat-wave during the summer 2009, which caused massive mortalities of corals, gorgonians, sponges and bivalves around Ischia (Rodolfo-Metalpa et al., 2011). This heat wave is equally recorded in the negative shift in shell $\delta^{18}\text{O}$ values directly prior to the transplantation (Fig. 10b, d).

Post-transplantation $\delta^{13}\text{C}_{\text{calcite}}$ becomes increasingly more positive. Towards the end of the transplantation experiment, $\delta^{13}\text{C}_{\text{calcite}}$ from the control site C is depleted by about 1 ‰ relative to seawater DIC (Fig. 10c), whilst it is enriched by more than 1 ‰ relative to seawater DIC at the experimental site B (Fig. 10a and Table 1). The conspicuous $\delta^{13}\text{C}$ shift is probably best understood in the context of sudden, transplantation-related changes in food availability and pop-

ulation density as well as seasonal changes in seawater DIC between harbour and experimental sites seawater. The offset between harbour seawater $\delta^{13}\text{C}_{\text{DIC}}$ and shell $\delta^{13}\text{C}_{\text{aragonite}}$ and $\delta^{13}\text{C}_{\text{calcite}}$ lie in the same overall range (0.2 to 1.5 ‰ for aragonite) as reported in Grossman and Ku (1986).

The maximum $\Delta^{18}\text{O}_{\text{shell}}$ in pre- and post-transplantation is 1.9 ‰. The shift from lighter to heavier $\delta^{18}\text{O}_{\text{shell}}$ ratios (Fig. 10b, d), reflects, in the view of the authors, only in part the abrupt transplantation change from warmer harbour temperatures to gradually cooler water masses at the test and control site (Fig. 2d). A heat wave in July and August 2009 with peak water temperatures of 26 °C stressed bivalves in Ischia harbour. Conspicuously, depleted $\delta^{18}\text{O}_{\text{shell}}$ ratios in pre-transplantation shell material (Fig. 10b and d) are evidence for this event. Applying the temperature equation of Anderson and Arthur (1983) for calcite to the *M. galloprovincialis* shell data, a pre-transplantation shell $\delta^{18}\text{O}$ ratio of -1.5 ‰ ($\delta^{18}\text{O}_{\text{seawater}}$ of 1.1 ‰ SMOW) corresponds to a seawater temperature of 27.6 °C, a value that is in reasonable agreement (+1.6 °C) with average august harbour water temperatures of 26 °C. After the transplantation in September, seawater temperatures at the control and the experimental site were still at 24 °C but fell to 20 °C during October. Peak December oxygen isotope values of 0.5 ‰ (Fig. 10b and d), in contrast, measured from shell calcite precipitated after the transplantation to control and experimental sites ($\delta^{18}\text{O}_{\text{seawater}}$ of 1.2 ‰ SMOW), correspond to calculated seawater temperature of 19 °C. This calculated value disagrees by 3 °C with measured seawater temperatures of 16 °C for December.

On the level of a working hypothesis, it seems likely, that changes in seawater pH (Bamber, 1987; Michaelidis et al., 2005; Berge et al., 2006; Beesley et al., 2008) influenced the shell oxygen isotope values, perhaps via calcification rates (Kleypas et al., 1999; Fabry et al., 2008) to some degree. Seawater pH, however, does not explain the observed isotope shifts in shells dislocated to the control site C that is characterized by a normal seawater pH. This is considered evidence that, under environmental stress such as the summer heat wave and the transplantation shock, *M. galloprovincialis* shell $\delta^{18}\text{O}$ is in disequilibrium with ambient seawater. The later observation is significant for shell calcite $\delta^{18}\text{O}$ seawater temperature reconstructions. In essence, shell $\delta^{18}\text{O}$ values overestimate seawater temperatures by approximately 1.5 to 3 °C.

Shell elemental compositions as shown in Figs. 7 and 8 are difficult to interpret. Differences in for example Mg abundance between calcite and aragonite are strongly controlled by the crystallographic properties of these carbonate materials (e.g. Okumura and Kitano, 1986; Dalbeck et al., 2006). In contrast to magnesium and calcium, however, sodium is more abundant in the nacreous layer compared to the calcite layer. Our results confirm the experiment of Okumura and Kitano (1986), which co-precipitated alkali ions with aragonite and calcite. They showed that sodium ions substitute for calcium in the aragonite lattice. The spatial differences

in Ca, Mg, Na and P elemental composition within either aragonite or calcite layers are probably meaningful on the level of biomineralization, i.e. the effect of acidified seawater, temperature and other environmental factors on element incorporation. Previous work has documented that Ca^{2+} and Mg^{2+} are transported across the epithelium via inter- and/or intra-cellular pathways (Watabe et al., 1990). Cations are either actively pumped across the cell membrane or move by passive diffusion through extracellular fluids to the site of calcification (Weiner and Dove, 2003; Addadi et al., 2006). At present, the authors accept that a detailed level of knowledge regarding the biologically controlled incorporation of elements in the shell of *M. galloprovincialis* is not reached and an in-depth interpretation of these data is beyond the scope of this paper.

The observed differences in the shell ultrastructure in specimen dislocated to experimental site B1 and control site C are significant and document the sensitivity of this previously underexplored proxy to environmental change. While the portions of the shell, that were biomineralized under normal seawater pH_T of 8.07 (control site C in Figs. 2d, 3a, b and 6c) are well ordered, the shell portions that precipitated under acidified seawater conditions (site B1; Fig. 2d, 4b and 5c) directly after the transplantation show a more unstructured shell microstructure than the control. Shell portions precipitated some weeks after the transplantation are rather well structured but contain spatially irregular shell portions with disordered calcite prisms (Fig. 3c, d). These detailed insights into the shell ultrastructure are equally encouraging and illustrated through the measured EBSD maps (Figs. 4 and 5).

Another important macroscopic feature refers to the aragonite or nacreous layer. In shell material from the acidified test environment B1, the aragonite layer is characterized by small, spatially isolated holes (diameters of ~ 0.1 mm), an overall reduced thickness and a dull surface (Fig. 1b). These dissolution effects may be caused by the acid base balance regulation of the mussel in acidified conditions (Michaelidis et al., 2005). Mussels that were transported to control C (pH_T 8.07) lack these features but are in contrast characterized by a highly lustrous nacreous layer.

*M. galloprovincialis*_{B1 and C} show both a distinct thinning of the calcite shell layer directly after the transplantation. A connection with the implementation process itself can not be excluded but the shells remain relatively thin after their adaptation to the new environment. Many independent factors, however, influence bivalve shell formation and thickness. Given that a shell thinning is present at sites with acidified and at sites with normal seawater pH, the relation between shell thickness and environmental factors is probably complex. All of these above features, structured versus unstructured shell organization, differences in the appearance of the nacreous layer, calcite layer thinning and marked changes in geochemical signature, have a considerable fossilization potential. These results are considered encouraging.

4.2 Environmental impact versus experimental bias

Mytilus shells are complex biomineral structures (Lowenstam and Weiner, 1989) precipitated under controlled extracellular processes (Crenshaw, 1980; Falini et al., 1996; Gotliv et al., 2003; Gaspard et al., 2008). Factors that affect the complex metabolic processes that in turn govern biomineralization include: (i) environment (Vander Putten et al., 2000) and here particularly seawater temperature (Grossman and Ku, 1986; Klein et al., 1996a; Bauwens et al., 2010), $\delta^{13}\text{C}$ of different carbon species in seawater (Dietzel and Kirchhoff, 2002; Hoefs, 2009 and references therein), salinity (Epstein and Mayeda, 1953; Bayne, 1976) and pH (Bamber, 1987; Michaelidis et al., 2005; Berge et al., 2006; Beesley et al., 2008); (ii) food availability (Gosling, 2003); and (iii) the degree of competition and population density (Gosling, 2003).

The potentially intricate combination of the above factors complicates the interpretation of geochemical and ultrastructural data shown here. This is because specimen of *M. galloprovincialis* were dislocated to environments not only characterized by different seawater temperatures and pH (Table 1) but where also exposed to sites with, in respect to their former harbour environment, different nutrient levels and seawater $\delta^{13}\text{C}_{\text{DIC}}$ and mussels experienced an abrupt change in population density. The abrupt change in the spatial orientation of calcite fibres c-axes across the transplantation suture shown in Fig. 4b is perhaps best explained by the transplantation shock because this suture line is present in samples dislocated to experimental (acidified) seawater site B1 as well as in such brought to control site C with normal pH. The transplantation shock therefore resulted in artefact features that are not expected in natural settings where environmental changes tend to be more gradual. This includes for example seasonal changes in seawater temperature, food availability but also gradual changes in population density.

The above consideration document the potential limitations of the field experimental setup applied here. First, our experiment was too short (68 days) to allow specimens to recover from the transplantation shock and to fully adapt to normal grow rates. Second, bivalves might have been stressed due to abnormally high seawater temperatures prior to the transplantation. Third, natural settings are by definition complex multi-factor systems. This background level of complexity, combined with experimental artefacts such as transplantation shock features limits the interpretation of geochemical and structural features observed to some degree. Culturing experiments, performed under constant environmental parameters and food availability (Thomsen and Melzner, 2010; Thomsen et al., 2010; Heinemann et al., 2011) are poor analogues of naturally complex environments but allow for a precise relation of specific environmental factors to textural or geochemical features observed in the test shells. In this sense, the outcome of the experiment shown here is considered a successful failure. Successful, as the data

clearly document the potential of combined geochemical and shell ultrastructure proxy analysis. A failure, as it is at present not possible to precisely allocate specific environmental parameters to specific geochemical or structural features.

5 Conclusions

Based on the data shown here, the following conclusions are drawn:

1. Live specimen of *M. galloprovincialis* were transplanted from Ischia harbour to nearby CO₂ vents and exposed to mean seawater pH_T 8.07 and 7.25. The shells responded with differential changes in shell carbon, oxygen and elemental composition, by a marked thinning of the calcite layer and by an – at least partial – lack of structure in the orientation of calcite prisms. In addition, the nacreous layer of mussels grown in experimental sites under acidified seawater was thin, dull and partially dissolved.
2. The marked trends in $\delta^{18}\text{O}$ across mussel shells grown after transplantation cannot be explained by seawater temperatures and pH differences alone. Oxygen-based seawater temperature calculations overestimate measured seawater temperatures by 1.5 to 3 °C. Pending more data, we suspect that environmental stress, and most dominantly seawater temperature and transplantation shock, affected mussel metabolism which in turn influenced the shell $\delta^{18}\text{O}$ ratios.
3. Pronounced shifts in $\delta^{13}\text{C}$ may reflect abrupt changes in food availability and population density when the mussels were transplanted to the CO₂ vent area. Remarkably, the pre- to post-transplantation $\Delta^{13}\text{C}_{\text{calcite}}$ of shells exposed to acidified experimental site seawater was about twice (4 ‰) that (2 ‰) found in shells precipitated from control site normal seawater pH. This points to an influence of seawater pH on bivalve metabolism and probably food availability that is again influenced by seawater pH.
4. Different shell layers, i.e. periostracum, aragonite and calcite layers show remarkable differences in both carbon and oxygen isotope values even when aragonite is normalized to calcite values. This notion questions the value of bulk data from bivalve shells.
5. Differences in shell elemental abundances in mussels exposed to acidified seawater at experimental site compared to normal conditions at control site are difficult to interpret. First order elemental differences are related to crystallographical differences between calcite and aragonite. Nevertheless, the spatial differences in Ca, Mg, Na and P elemental composition within one shell layer are highly complex and probably meaningful on the level of metabolic controls during biomineralization.

6. We have documented the successful application of a combined geochemical and shell ultrastructural/textural proxy analysis from complex natural archives. The transplantation shock clearly recorded in the mussel shells is a problem and suggests that specimen must be kept several months at test sites before they adapt to the new environment. Our field experiments show that caution is required when using bivalve shells to interpret past ocean acidification events as shells can respond to a range of factors along with the effects of high CO₂.
7. It is proposed that the combination of field experiments and laboratory cultures will lead to an improved understanding of factors affecting shell growth and its use in interpretations of ocean acidification events.

Supplementary material related to this article is available online at: <http://www.biogeosciences.net/9/1897/2012/bg-9-1897-2012-supplement.pdf>.

Acknowledgements. This is a contribution to BioAcid. We wish to thank R. Enders (LMU Munich) and the laboratory staff at the Ruhr University for analytical support. We thank Andreas Götz for his support and image analysis program. We especially thank Dorothee Hippler for the discussions and insights into the topic. The project has been supported by FP7 EU MedSeA (265103) and EU MARES. We thankfully acknowledge the support of Federal Ministry of Education and Research (BMBF; FKZ 03F0608H).

Edited by: C. P. Slomp

References

- Addadi, L., Joester, D., Nudelman, F., and Weiner, S.: Mollusk shell formation: A source of new concepts for understanding biomineralization processes, *Chemistry*, 12, 980–987, doi:10.1002/chem.200500980, 2006.
- Aguirre, M. L., Perez, S. I., and Sirch, Y. N.: Morphological variability of *brachidontes swainson* (bivalvia, *Mytilidae*) in the marine Quaternary of Argentina (SW Atlantic), *Palaeogeogr. Palaeoclimatol.*, 239, 100–125, doi:10.1016/j.palaeo.2006.01.019, 2006.
- Anderson, T. F. and Arthur, M. A.: Stable isotopes of oxygen and carbon and their application to sedimentologic and paleoenvironmental problems, 10. *Society of Sedimentary Geology*, 151 pp., 1983.
- Aral, O.: Growth of the Mediterranean mussel (*Mytilus galloprovincialis* lam., 1819) on ropers in the Black Sea, Turkey, *Turk. J. Vet. Anim. Sci.*, 23, 183–189, 1999.
- Aubry, M. P., Ouda, K., Dupuis, C., Berggren, W. A., and Van Couvering, J. A.: The Global Standard Stratotype-section and Point (GSSP) for the base of the Eocene series in the Dababiya section (Egypt), *Episodes*, 30, 271–286, 2007.

- Bamber, R. N.: The effects of acidic sea-water on young carpet-shell clams *Venerupis-decussata* (l) (mollusca, *Veneracea*), *J. Exp. Mar. Biol. Ecol.*, 108, 241–260, doi:10.1016/0022-0981(87)90088-8, 1987.
- Bauwens, M., Ohlsson, H., Barbé, K., Beelaerts, V., Schoukens, J., and Dehairs, F.: A nonlinear multi-proxy model based on manifold learning to reconstruct water temperature from high resolution trace element profiles in biogenic carbonates, *Geosci. Model Dev.*, 3, 653–667, doi:10.5194/gmd-3-653-2010, 2010.
- Bayne, B. L.: Marine mussels, their ecology and physiology, in: *International Biological Programme Synthesis Series*, Cambridge University Press, Cambridge, UK, 523, 47–48, 200–205, 1976.
- Beesley, A., Lowe, D. M., Pascoe, C. K., and Widdicombe, S.: Effects of CO₂-induced seawater acidification on the health of *Mytilus edulis*, *Clim. Res.*, 37, 215–225, doi:10.3354/cr00765, 2008.
- Berge, J. A., Bjerkeng, B., Pettersen, O., Schaanning, M. T., and Oxnevad, S.: Effects of increased sea water concentrations of CO₂ on growth of the bivalve *Mytilus edulis* l, *Chemosphere*, 62, 681–687, doi:10.1016/j.chemosphere.2005.04.111, 2006.
- Buick, D. P. and Ivany, L. C.: 100 years in the dark: Extreme longevity of Eocene bivalves from Antarctica, *Geology*, 32, 921–924, doi:10.1130/g20796.1, 2004.
- Caldeira, K. and Wickett, M. E.: Anthropogenic carbon and ocean pH, *Nature*, 425, 365–365, doi:10.1038/425365a, 2003.
- Carroll, M. L., Johnson, B. J., Henkes, G. A., McMahon, K. W., Voronkov, A., Ambrose, W. G., and Denisenko, S. G.: Bivalves as indicators of environmental variation and potential anthropogenic impacts in the southern Barents Sea, *Mar. Pollut. Bull.*, 59, 193–206, doi:10.1016/j.marpolbul.2009.02.022, 2009.
- Checa, A.: A new model for periostracum and shell formation in *Unionidae* (bivalvia, mollusca), *Tissue Cell*, 32, 405–416, doi:10.1054/tice.2000.0129, 2000.
- Cigliano, M., Gambi, M. C., Rodolfo-Metalpa, R., Patti, F. P., and Hall-Spencer, J. M.: Effects of ocean acidification on invertebrate settlement at volcanic CO₂ vents, *Mar. Biol.*, 157, 2489–2502, doi:10.1007/s00227-010-1513-6, 2010.
- Crenshaw, M. A.: Mechanisms of shell formation and dissolution, in: *Skeletal growth of aquatic organisms*, edited by: Rhods, D. C. and Lutz, R. A., Plenum Publishing Corporation, New York, 115–132, 1980.
- Dalbeck, P., England, J., Cusack, M., Lee, M. R., and Fallick, A. E.: Crystallography and chemistry of the calcium carbonate polymorph switch in *M. edulis* shells, *Eur. J. Mineral.*, 18, 601–609, doi:10.1127/0935-1221/2006/0018-0601, 2006.
- Davies, A. J., Roberts, J. M., and Hall-Spencer, J.: Preserving deep-sea natural heritage: Emerging issues in offshore conservation and management, *Biol. Conserv.*, 138, 299–312, doi:10.1016/j.biocon.2007.05.011, 2007.
- Dettman, D. L. and Lohmann, K. C.: Microsampling carbonates for stable isotope and minor element analysis – physical separation of samples on a 20 µm scale, *J. Sediment. Res. A*, 65, 566–569, 1995.
- Dias, B. B., Hart, B., Smart, C. W., and Hall-Spencer, J. M.: Modern seawater acidification: The response of foraminifera to high-CO₂ conditions in the Mediterranean Sea, *J. Geol. Soc. London*, 167, 843–846, doi:10.1144/0016-76492010-050, 2010.
- Dietzel, M. and Kirchhoff, T.: Stable isotope ratios and the evolution of acidulous ground water, *Aquat. Geochem.*, 8, 229–254, doi:10.1023/B:AQUA.0000003724.43004.1e, 2002.
- Elliot, M., deMenocal, P. B., Linsley, B. K., and Howe, S. S.: Environmental controls on the stable isotopic composition of *Mercenaria mercenaria*: Potential application to paleo-environmental studies, *Geochem. Geophys. Geosy.*, 4, 1–16, doi:10.1029/2002gc000425, 2003.
- Ellis, R. P., Bersey, J., Rundle, S. D., Hall-Spencer, J. M., and Spicer, J. I.: Subtle but significant effects of CO₂ acidified seawater on embryos of the intertidal snail, *Littorina obtusata*, *Aquat. Biol.*, 5, 41–48, doi:10.3354/ab00118, 2009.
- Elorza, J. and GarciaGarmilla, F.: Petrological and geochemical evidence for diagenesis of inoceramid bivalve shells in the Plentzia formation (Upper Cretaceous, Basque-Cantabrian region, Northern Spain), *Cretaceous Res.*, 17, 479–503, doi:10.1006/cres.1996.0029, 1996.
- Engel, A., Zondervan, I., Aerts, K., Beaufort, L., Benthien, A., Chou, L., Delille, B., Gattuso, J. P., Harlay, J., Heemann, C., Hoffmann, L., Jacquet, S., Nejstgaard, J., Pizay, M. D., Rochelle-Newall, E., Schneider, U., Terbruggen, A., and Riebesell, U.: Testing the direct effect of CO₂ concentration on a bloom of the coccolithophorid *Emiliania huxleyi* in mesocosm experiments, *Limnol. Oceanogr.*, 50, 493–507, doi:10.4319/lo.2005.50.2.0493, 2005.
- Epstein, S. and Mayeda, T.: Variation of o-18 content of waters from natural sources, *Geochim. Cosmochim. Ac.*, 4, 213–224, doi:10.1016/0016-7037(53)90051-9, 1953.
- Fabry, V. J., Seibel, B. A., Feely, R. A., and Orr, J. C.: Impacts of ocean acidification on marine fauna and ecosystem processes, *Ices J. Mar. Sci.*, 65, 414–432, doi:10.1093/icesjms/fsn048, 2008.
- Falini, G., Albeck, S., Weiner, S., and Addadi, L.: Control of aragonite or calcite polymorphism by mollusk shell macromolecules, *Science*, 271, 67–69, doi:10.1126/science.271.5245.67, 1996.
- Fine, M. and Tchernov, D.: Ocean acidification and Scleractinian corals, *Science*, 317, 1032–1033, 2007.
- Foster, L. C., Allison, N., Finch, A. A., Andersson, C., and Ninemann, U. S.: Controls on delta δ¹⁸O and delta δ¹³C profiles within the aragonite bivalve *Arctica islandica*, Holocene, 19, 549–558, doi:10.1177/0959683609104028, 2009.
- Gaspard, D., Marin, F., Guichard, N., Morel, S., Alcaraz, G., and Luquet, G.: Shell matrices of recent rhynchonelliform brachiopods: Microstructures and glycosylation studies, *Earth Env. Sci. T. R. So.*, 98, 415–424, doi:10.1017/s1755691007078401, 2008.
- Gazeau, F., Quiblier, C., Jansen, J. M., Gattuso, J. P., Middelburg, J. J., and Heip, C. H. R.: Impact of elevated CO₂ on shellfish calcification, *Geophys. Res. Lett.*, 34, 1–5, doi:10.1029/2006GL028554, 2007.
- Gibbs, S. J., Bown, P. R., Sessa, J. A., Bralower, T. J., and Wilson, P. A.: Nannoplankton extinction and origination across the Paleocene-Eocene Thermal Maximum, *Science*, 314, 1770–1773, doi:10.1126/science.1133902, 2006.
- Gibbs, S. J., Stoll, H. M., Bown, P. R., and Bralower, T. J.: Ocean acidification and surface water carbonate production across the Paleocene-Eocene Thermal Maximum, *Earth Planet. Sc. Lett.*, 295, 583–592, doi:10.1016/j.epsl.2010.04.044, 2010.
- Gillikin, D. P., Dehairs, F., Lorrain, A., Steenmans, D., Baeyens, W., and Andre, L.: Barium uptake into the shells of the common mussel (*Mytilus edulis*) and the potential for estuarine

- paleo-chemistry reconstruction, *Geochim. Cosmochim. Ac.*, 70, 395–407, doi:10.1016/j.gca.2005.09.015, 2006a.
- Gillikin, D. P., Lorrain, A., Bouillon, S., Willenz, P., and Dehairs, F.: Stable carbon isotopic composition of *Mytilus edulis* shells: Relation to metabolism, salinity, delta C-13(dic) and phytoplankton, *Org. Geochem.*, 37, 1371–1382, doi:10.1016/j.orggeochem.2006.03.008, 2006b.
- Giusberti, L., Rio, D., Agnini, C., Backman, J., Fornaciari, E., Tateo, F., and Oddone, M.: Mode and tempo of the Paleocene-Eocene Thermal Maximum in an expanded section from the Venetian pre-Alps, *Geol. Soc. Am. Bull.*, 119, 391–412, doi:10.1130/b25994.1, 2007.
- Gomez-Alday, J. J. and Elorza, J.: Diagenesis, regular growth and records of seasonality in inoceramid bivalve shells from mid-Maastrichtian hemipelagic beds of the Bay of Biscay, *Neth. J. Geosci.*, 82, 289–301, 2003.
- Gosling, E.: Bivalve molluscs – biology, ecology and culture, Fishing News Books, Blackwell Publishers, 44–50, 182–184, 188–189, 2003.
- Gotliv, B. A., Addadi, L., and Weiner, S.: Mollusk shell acidic proteins, in: Search of individual functions, *Chembiochem*, 4, 522–529, doi:10.1002/cbic.200200548, 2003.
- Grossman, E. L. and Ku, T. L.: Oxygen and carbon isotope fractionation in biogenic aragonite: Temperature effects, *Chem. Geol.*, 59, 59–74, doi:10.1016/0009-2541(86)90044-6, 1986.
- Guinotte, J. M. and Fabry, V. J.: Ocean acidification and its potential effects on marine ecosystems, *Ann. Ny. Acad. Sci.*, 1134, 320–342, doi:10.1196/annals.1439.013, 2008.
- Gutowska, M. A., Melzner, F., Portner, H. O., and Meier, S.: Cuttlebone calcification increases during exposure to elevated seawater pCO₂ in the cephalopod *Sepia officinalis*, *Mar. Biol.*, 157, 1653–1663, doi:10.1007/s00227-010-1438-0, 2010.
- Hall-Spencer, J. M., Rodolfo-Metalpa, R., Martin, S., Ransome, E., Fine, M., Turner, S. M., Rowley, S. J., Tedesco, D., and Buia, M. C.: Volcanic carbon dioxide vents show ecosystem effects of ocean acidification, *Nature*, 454, 96–99, doi:10.1038/nature07051, 2008.
- Heinemann, A., Fietzke, J., Eisenhauer, A., and Zumholz, K.: Modification of Ca isotope and trace metal composition of the major matrices involved in shell formation of *Mytilus edulis*, *Geochem. Geophys. Geosy.*, 9, 1–8, doi:10.1029/2007gc001777, 2008.
- Heinemann, A., Hiebenthal, C., Fietzke, J., Eisenhauer, A., and Wahl, M.: Disentangling the biological and environmental control of *M. edulis* shell chemistry, *Geochem. Geophys. Geosy.*, 12, Q05012, doi:10.1029/2011GC003673, 2011.
- Hietanen, B., Sunila, I., and Kristoffersson, R.: Toxic effects of zinc on the common mussel *Mytilus edulis* L. (bivalvia) in brackish water. 1. Physiological and histopathological studies, *Ann. Zool. Fenn.*, 25, 341–347, 1988.
- Hippler, D., Buhl, D., Witbaard, R., Richter, D. K., and Immenhauser, A.: Towards a better understanding of magnesium-isotope ratios from marine skeletal carbonates, *Geochim. Cosmochim. Ac.*, 73, 6134–6146, doi:10.1016/j.gca.2009.07.031, 2009.
- Hoefs, J.: Stable isotope geochemistry (6th Edn.), Springer, New York, Heidelberg & Berlin, 2009.
- Hoegh-Guldberg, O., Mumby, P. J., Hooten, A. J., Steneck, R. S., Greenfield, P., Gomez, E., Harvell, C. D., Sale, P. F., Edwards, A. J., Caldeira, K., Knowlton, N., Eakin, C. M., Iglesias-Prieto, R., Muthiga, N., Bradbury, R. H., Dubi, A., and Hatzioles, M. E.: Coral reefs under rapid climate change and ocean acidification, *Science*, 318, 1737–1742, doi:10.1126/science.1152509, 2007.
- Iglesias-Rodriguez, M. D., Halloran, P. R., Rickaby, R. E. M., Hall, I. R., Colmenero-Hidalgo, E., Gittins, J. R., Green, D. R. H., Tyrrell, T., Gibbs, S. J., von Dassow, P., Rehm, E., Armbrust, E. V., and Boessenkool, K. P.: Phytoplankton calcification in a high-CO₂ world, *Science*, 320, 336–340, doi:10.1126/science.1154122, 2008.
- Immenhauser, A., Nägler, T. F., Steuber, T., and Hippler, D.: A critical assessment of mollusk O-18/O-16, Mg/Ca, and Ca-44/Ca-40 ratios as proxies for cretaceous seawater temperature seasonality, *Palaeogeogr. Palaeoclimatol.*, 215, 221–237, doi:10.1016/j.palaeo.2004.09.005, 2005.
- Immenhauser, A., Holmden, C., and Patterson, W. P.: Interpreting the carbon-isotope record of ancient shallow epeiric seas: Lessons from the recent, in: Dynamics of epeiric seas, edited by: Pratt, B. R. and Holmden, C., Geological Association of Canada Special Publication, 135–174, 2008.
- Kennedy, W. J., Taylor, J. D., and Hall, A.: Environmental and biological controls on bivalve shell mineralogy, *Biological Review of the Cambridge Philosophical Society*, 44, 499–530, doi:10.1111/j.1469-185X.1969.tb00610.x, 1969.
- Kisakürek, B., Eisenhauer, A., Böhm, F., Hathorne, E. C., and Erez, J.: Controls on calcium isotope fractionation in cultured planktic foraminifera, *Globigerinoides ruber* and *Globigerinella siphonifera*, *Geochim. Cosmochim. Ac.*, 75, 427–443, doi:10.1016/j.gca.2010.10.015, 2011.
- Klein, R. T., Lohmann, K. C., and Thayer, C. W.: Bivalve skeletons record sea-surface temperature and delta O-18 via Mg/Ca and O-18/O-16 ratios, *Geology*, 24, 415–418, doi:10.1130/0091-7613(1996)024<0415:BSRSST>2.3.CO;2, 1996a.
- Klein, R. T., Lohmann, K. C., and Thayer, C. W.: Sr/Ca and C-13/C-12 ratios in skeletal calcite of *Mytilus trossulus*: Covariation with metabolic rate, salinity, and carbon isotopic composition of seawater, *Geochim. Cosmochim. Ac.*, 60, 4207–4221, doi:10.1016/S0016-7037(96)00232-3, 1996b.
- Kleypas, J. A., Buddemeier, R. W., Archer, D., Gattuso, J. P., Langdon, C., and Opdyke, B. N.: Geochemical consequences of increased atmospheric carbon dioxide on coral reefs, *Science*, 284, 118–120, doi:10.1126/science.284.5411.118, 1999.
- Koehn, R. K.: The genetics and taxonomy of species in the genus *mytilus*, *Aquaculture*, 94, 125–145, 1991.
- Kroeker, K. J., Micheli, F., Gambi, M. C., and Martz, T. R.: Divergent ecosystem responses within a benthic marine community to ocean acidification, *PNAS*, 108, 14515–14520, doi:10.1073/pnas.1107789108, 2011.
- Kump, L. R., Bralower, T. J., and Ridgwell, A.: Ocean acidification in deep time, *Oceanography*, 22, 94–107, doi:10.5670/oceanog.2009.100, 2009.
- Latal, C., Piller, W. E., and Harzhauser, M.: Shifts in oxygen and carbon isotope signals in marine molluscs from the central Paratethys (Europe) around the lower/middle Miocene transition, *Palaeogeogr. Palaeoclimatol.*, 231, 347–360, doi:10.1016/j.palaeo.2005.08.008, 2006.
- Lecuyer, C., Reynard, B., and Martineau, F.: Stable isotope fractionation between mollusc shells and marine waters from Martinique island, *Chem. Geol.*, 213, 293–305, doi:10.1016/j.chemgeo.2004.02.001, 2004.

- Lopez Correa, M., Freiwald, A., Hall-Spencer, J., Taviani, M., and Roberts, J. M.: Distribution and habitats of *Acesta excavata* (bivalvia: Limidae) with new data on its shell ultrastructure, Cold-water corals and ecosystems [Erlangen Earth Conference Series], 173–205, doi:10.1007/3-540-27673-4_9, 2005.
- Lorens, R. B. and Bender, M. L.: Physiological exclusion of magnesium from *Mytilus edulis* calcite, *Nature*, 269, 793–794, doi:10.1038/269793a0, 1977.
- Lowenstam, H. A. and Weiner, S.: On biomineralization, in *Biomineralization: Chemical and Biochemical Perspectives*, Oxford University Press, Inc., New York, 27–49, 99–110, 1989.
- Lüthi, D., Le Floch, M., Bereiter, B., Blunier, T., Barnola, J. M., Siegenthaler, U., Raynaud, D., Jouzel, J., Fischer, H., Kawamura, K., and Stocker, T. F.: High-resolution carbon dioxide concentration record 650,000–800,000 years before present, *Nature*, 453, 379–382, doi:10.1038/nature06949, 2008.
- Manzello, D. P., Kleypas, J. A., Budd, D. A., Eakin, C. M., Glynn, P. W., and Langdon, C.: Poorly cemented coral reefs of the eastern tropical pacific: Possible insights into reef development in a high-CO₂ world, *P. Natl. Acad. Sci. USA*, 105, 10450–10455, doi:10.1073/pnas.0712167105, 2008.
- Marin, F. and Luquet, G.: Molluscan shell proteins, *C. R. Palevol*, 3, 469–492, 2004.
- Martin, S., Rodolfo-Metalpa, R., Ransome, E., Rowley, S., Buia, M. C., Gattuso, J. P., and Hall-Spencer, J.: Effects of naturally acidified seawater on seagrass calcareous epibionts, *Biol. Letters*, 4, 689–692, doi:10.1098/rsbl.2008.0412, 2008.
- Michaelidis, B., Ouzounis, C., Paleras, A., and Portner, H. O.: Effects of long-term moderate hypercapnia on acid-base balance and growth rate in marine mussels *Mytilus galloprovincialis*, *Mar. Ecol.-Prog. Ser.*, 293, 109–118, doi:10.3354/meps293109, 2005.
- Mutterlose, J., Linnert, C., and Norris, R.: Calcareous nanofossils from the Paleocene-Eocene Thermal Maximum of the equatorial Atlantic (ODP site 1260b): Evidence for tropical warming, *Mar. Micropaleontol.*, 65, 13–31, doi:10.1016/j.marmicro.2007.05.004, 2007.
- Okumura, M. and Kitano, Y.: Coprecipitation of alkali metal ions with calcium carbonate, *Geochim. Cosmochim. Ac.*, 50, 49–58, doi:10.1016/0016-7037(86)90047-5, 1986.
- Orr, J. C., Fabry, V. J., Aumont, O., Bopp, L., Doney, S. C., Feely, R. A., Gnanadesikan, A., Gruber, N., Ishida, A., Joos, F., Key, R. M., Lindsay, K., Maier-Reimer, E., Matear, R., Monfray, P., Mouchet, A., Najjar, R. G., Plattner, G. K., Rodgers, K. B., Sabine, C. L., Sarmiento, J. L., Schlitzer, R., Slater, R. D., Totterdell, I. J., Weirig, M. F., Yamanaka, Y., and Yool, A.: Anthropogenic ocean acidification over the twenty-first century and its impact on calcifying organisms, *Nature*, 437, 681–686, doi:10.1038/nature04095, 2005.
- Pierre, C.: The oxygen and carbon isotope distribution in the Mediterranean water masses, *Mar. Geol.*, 153, 41–55, doi:10.1016/s0025-3227(98)00090-5, 1999.
- Pouchou, J. L. and Pichoir, F.: A new model for quantitative x-ray-microanalysis. 2. Application to in-depth analysis of heterogeneous samples, *Rech. Aerospatiale*, 5, 349–367, 1984.
- Raffi, I., Backman, J., and Palike, H.: Changes in calcareous nanofossil assemblages across the Paleocene/Eocene transition from the paleo-equatorial Pacific Ocean, *Palaeogeogr. Palaeoclimatol.*, 226, 93–126, doi:10.1016/j.palaeo.2005.05.006, 2005.
- Ragland, P. C., Pilkey, O. H., and Blackwelder, B. W.: Diagenetic changes in the elemental composition of uncrystallized mollusk shells, *Chem. Geol.*, 25, 123–134, doi:10.1016/0009-2541(79)90088-3, 1979.
- Riebesell, U., Schulz, K. G., Bellerby, R. G. J., Botros, M., Fritsche, P., Meyerhofer, M., Neill, C., Nondal, G., Oschlies, A., Wohlers, J., and Zollner, E.: Enhanced biological carbon consumption in a high CO₂ ocean, *Nature*, 450, 545–510, doi:10.1038/nature06267, 2007.
- Rodolfo-Metalpa, R., Lombardi, C., Cocito, S., Hall-Spencer, J., and Gambi, M. C.: Effects of ocean acidification and high temperatures on the bryozoan *Myriapora truncata* and natural CO₂ vents, *Mar. Ecol.*, 31, 447–456, doi:10.1111/j.1439-0485.2009.00354.x, 2010.
- Rodolfo-Metalpa, R., Houlbrèque, F., Tambutté, E., Boisson, F., Baggini, C., Patti, F. P., Jeffree, R., Fine, M., Foggo, A., Gattuso, J.-P., and Hall-Spencer, J. M.: Coral and mollusc resistance to ocean acidification adversely affected by warming, *Nature Climate Change Letters*, 1, 308–312, doi:10.1038/NCLIMATE1200, 2011.
- Röhl, U., Westerhold, T., Bralower, T. J., and Zachos, J. C.: On the duration of the Paleocene-Eocene Thermal Maximum (PETM), *Geochim. Geophys. Geos.*, 8, 1–13, doi:10.1029/2007GC001784, 2007.
- Rubinson, M. and Clayton, R. N.: Carbon-13 fractionation between aragonite and calcite, *Geochim. Cosmochim. Ac.*, 33, 997–1002, 1969.
- Russell, A. D., Honisch, B., Spero, H. J., and Lea, D. W.: Effects of seawater carbonate ion concentration and temperature on shell U, Mg, and Sr in cultured planktonic foraminifera, *Geochim. Cosmochim. Ac.*, 68, 4347–4361, doi:10.1016/j.gca.2004.03.013, 2004.
- Scheibner, C. and Speijer, R. P.: Late Paleocene-early Eocene tethyan carbonate platform evolution – a response to long- and short-term paleoclimatic change, *Earth-Sci. Rev.*, 90, 71–102, doi:10.1016/j.earscirev.2008.07.002, 2008.
- Shumway, S. E.: Effect of salinity fluctuation on osmotic-pressure and Na⁺, Ca²⁺ and Mg²⁺ ion concentrations in hemolymph of bivalve mollusks, *Mar. Biol.*, 41, 153–177, doi:10.1007/BF00394023, 1977.
- Sluijs, A., Brinkhuis, H., Schouten, S., Bohaty, S. M., John, C. M., Zachos, J. C., Reichert, G. J., Damste, J. S. S., Crouch, E. M., and Dickens, G. R.: Environmental precursors to rapid light carbon injection at the Palaeocene/Eocene boundary, *Nature*, 450, 1218–1215, doi:10.1038/nature06400, 2007.
- Solomon, S., Plattner, G. K., Knutti, R., and Friedlingstein, P.: Irreversible climate change due to carbon dioxide emissions, *P. Natl. Acad. Sci. USA*, 106, 1704–1709, doi:10.1073/pnas.0812721106, 2009.
- Tarutani, T., Clayton, R. N., and Mayeda, T. K.: The effect of polymorphism and magnesium substitution on oxygen isotope fractionation between calcium carbonate and water, *Geochim. Cosmochim. Ac.*, 33, 987–996, 1969.
- Tedesco, D.: Chemical and isotopic investigations of fumarolic gases from Ischia Island (Southern Italy): Evidences of magmatic and crustal contribution, *J. Volcanol. Geoth. Res.*, 74, 233–242, doi:10.1016/S0377-0273(96)00030-3, 1996.
- Thomsen, J. and Melzner, F.: Moderate seawater acidification does not elicit long-term metabolic depression in the blue mussel

- Mytilus edulis*, Mar. Biol., 157, 2667–2676, doi:10.1007/s00227-010-1527-0, 2010.
- Thomsen, J., Gutowska, M. A., Saphörster, J., Heinemann, A., Trübenbach, K., Fietzke, J., Hiebenthal, C., Eisenhauer, A., Körtzinger, A., Wahl, M., and Melzner, F.: Calcifying invertebrates succeed in a naturally CO₂-rich coastal habitat but are threatened by high levels of future acidification, Biogeosciences, 7, 3879–3891, doi:10.5194/bg-7-3879-2010, 2010.
- Tynan, S., Opkyke, B. N., Ellis, D., and Beavis, S.: A history of heavy metal pollution recorded in the shell of *Mytilus edulis*, Geochim. Cosmochim. Ac., 70, A662–A662, doi:10.1016/j.gca.2006.06.1235, 2006.
- Vander Putten, E., Dehairs, F., Keppens, E., and Baeyens, W.: High resolution distribution of trace elements in the calcite shell layer of modern *Mytilus edulis*: Environmental and biological controls, Geochim. Cosmochim. Ac., 64, 997–1011, doi:10.1016/S0016-7037(99)00380-4, 2000.
- Wanamaker, A. D., Kreutz, K. J., Borns, H. W., Introne, D. S., Feindel, S., Funder, S., Rawson, P. D., and Barber, B. J.: Experimental determination of salinity, temperature, growth, and metabolic effects on shell isotope chemistry of *Mytilus edulis* collected from Maine and Greenland, Paleoceanography, 22, 1–12, doi:10.1029/2006pa001352, 2007.
- Watabe, N., Kingsley, R. J., and Crick, R. E.: Extra-, inter-, and intracellular mineralization in invertebrates and algae, Origin, evolution and modern aspects of biomineralization in plants and animals, 209–223, 1990.
- Weiner, S. and Dove, P. M.: An overview of biomineralization processes and the problem of the vital effect, Biomineralization, 54, 1–29, doi:10.2113/0540001, 2003.
- Westerhold, T., Rohl, U., Laskar, J., Raffi, I., Bowles, J., Lourens, L. J., and Zachos, J. C.: On the duration of magnetochrons C24r and C25n and the timing of early Eocene global warming events: Implications from the ocean drilling program leg 208 Walvis Ridge depth transect, Paleoceanography, 22, 1–19, doi:10.1029/2006pa001322, 2007.
- Witbaard, R., Jenness, M. I., Vanderborg, K., and Ganssen, G.: Verification of annual growth increments in *Arctica islandica* l. From the North Sea by means of oxygen and carbon isotopes, Neth. J. Sea Res., 33, 91–101, doi:10.1016/0077-7579(94)90054-X, 1994.
- Zachos, J. C., Rohl, U., Schellenberg, S. A., Sluijs, A., Hodell, D. A., Kelly, D. C., Thomas, E., Nicolo, M., Raffi, I., Lourens, L. J., McCarren, H., and Kroon, D.: Rapid acidification of the ocean during the Paleocene-Eocene Thermal Maximum, Science, 308, 1611–1615, doi:10.1126/science.1109004, 2005.
- Zeebe, R. E. and Ridgwell, A.: Past changes in ocean carbonate chemistry, in: Ocean acidification, edited by: Gattuso, J.-P. and Hansson, L., Oxford University Press, Oxford, 21–40, 2011.